INVITED PAPER

Collaborative Sensor Network Localization: Algorithms and Practical Issues

This paper surveys collaborative localization with an emphasis on algorithms and practical issues in applications for 5G and IoT networks.

By R. Michael Buehrer, *Fellow IEEE*, Henk Wymeersch, *Member IEEE*, and Reza Monir Vaghefi, *Member IEEE*

ABSTRACT | Emerging communication network applications including fifth-generation (5G) cellular and the Internet-of-Things (IoT) will almost certainly require location information at as many network nodes as possible. Given the energy requirements and lack of indoor coverage of Global Positioning System (GPS), collaborative localization appears to be a powerful tool for such networks. In this paper, we survey the state of the art in collaborative localization with an eye toward 5G cellular and IoT applications. In particular, we discuss theoretical limits, algorithms, and practical challenges associated with collaborative localization based on range-based as well as range-angle-based techniques.

KEYWORDS | 5G; collaborative localization; cooperative localization; DOA; IoT; localization; sensor networks; sensor network localization; ranging; TOA

I. INTRODUCTION

Radio localization has a long history, with the best known example being satellite-based localization, such as Global Positioning System (GPS) and Galileo [1]. These systems rely on low-rate signals from a constellation of synchronized satellites, allowing the receiver to simultaneously localize itself and synchronize its clock using time-of-arrival (TOA) measurements.[1] As GPS-based localization has a number of drawbacks, primarily related to coverage and power consumption, it is often complemented by terrestrial techniques. Among those, three technologies stand out: cellular, WiFi, and ultrawideband (UWB). Cellular localization (the primary backup to GPS in smartphones) was primarily implemented for emergency call localization, and has undergone various changes across different generations of cellular system development. Current long-term evolution (LTE) systems rely on time-difference-of-arrival (TDOA) measurements using synchronized base stations, from which the network then computes the user's position, with accuracies ranging from 10 to 200 m [2]. Further accuracy improvements to indoor localization are possible with WiFi-based localization. In contrast to the time-based measurements in GPS and cellular localization, WiFi localization relies on signal strength maps, thus requiring periodic surveying. However, for high-precision localization (below 10 cm), conventional WiFi is not suitable and dedicated technologies are preferred. In particular, UWB has found niche application, due to its large available bandwidth [3]. UWB localization systems exist with TDOA (requiring synchronized anchors) or two-way TOA (TW-TOA) ranging. In TW-TOA, no *a priori* synchronization is needed, so that the network can operate in *ad hoc* mode, without the need for a fixed anchor deployment [4]. With *ad hoc* localization come challenges of scalability in terms of communication with anchors, information sharing, and computation. These are addressed in the collaborative localization paradigm.

In collaborative (or cooperative) localization [5]–[7], direct internode measurements support the localization, providing improvements both in terms of coverage and

[1]GPS technically uses TOA measurements with TDOA positioning given the lack of synchronization between the transmitter and the receiver.

Manuscript received August 7, 2017; revised February 27, 2018; accepted April 5, 2018. Date of publication May 15, 2018; date of current version May 24, 2018. The work of R. M. Buehrer was supported by the National Science Foundation under Grants 0515019 and 0802112 and the Bradley Foundation. The work of H. Wymeersch was supported by the European Union (EU) H2020 projects HIGHTS (High Precision Positioning for Cooperative ITS Applications under Grant MG-3.5a-2014-636537) and 5GCAR, as well as the VINNOVA COPPLAR project, funded under Strategic Vehicle Research and Innovation Grant 2015-04849. *(Corresponding author: R. Michael Buehrer.)*

R. M. Buehrer is with the Department of Electrical and Computer Engineering, Virginia Tech, Blacksburg, VA 24060 USA and also with the Wireless @ Virginia Tech, Blacksburg, VA 24060 USA (e-mail: buehrer@vt.edu).

H. Wymeersch is with the Department of Electrical Engineering, Chalmers University of Technology, 412 58 Göteborg, Sweden (e-mail: henkw@chalmers.se).

R. M. Vaghefi is with Blue Danube Systems, Santa Clara, CA 95054 USA (e-mail: vaghefi@vt.edu).

Digital Object Identifier: 10.1109/JPROC.2018.2829439

accuracy. Collaborative localization can be directly combined with UWB TW-TOA as well as device-to-device (D2D) LTE and fifth-generation (5G) communication [8], [9]. The benefits of collaboration have been quantified both theoretically and algorithmically. Analysis based on Fisher information has led to, for example, a demonstration of the benefit of collaboration [10], insights into the fundamental nature of collaboration and the scaling with network size [11], [12], power allocation [13], [14], anchor placement [15], and neighbor selection [16]. Building on these fundamental insights, a large number of localization algorithms have been developed depending on the measurement type used, where the localization computation is performed, the order of localization, and the objective function being optimized [7]. Despite the theoretical studies indicating clear benefits of collaborative localization and the existence of powerful distributed algorithms that are able to harness the additional information from internode measurements, there have been few practical deployments. This is mainly due to the fundamental challenge of *ad hoc* networking: orchestrating efficient communication in *ad hoc* networks is still notoriously hard. This is especially important for time-based distance measurements, where even small delays can lead to large ranging errors and where measurements must be processed in a timely manner. Though delays are less critical for static networks, in dynamic networks, the localization process must complete sufficiently fast with respect to node mobility.

These hurdles are expected to be removed once 5G networks are available. For enhanced mobile broadband and ultrareliable and low latency communications, such networks can offer large bandwidths (and thus precise ranging), large arrays (enabling accurate angle estimation), as well as a communication protocol for efficient D2D links between relatively powerful devices. Such links can be controlled by base stations, thus avoiding the delay issues that have plagued early generations of collaborative localization. In addition to 5G networks, Internet-of-Things (IoT) applications represent another emerging area where the need for location information is strong. For IoT applications where location is needed (or beneficial), a UWB-based physical layer (or other wideband technique) is a likely candidate. Further, collaborative localization appears to be a technique which will be extremely useful in these applications. Given the high probability in IoT applications that GPS will not be available at all nodes (due either to coverage limitations or computational complexity limitations), collaborative localization is an attractive technology. Further, IoT networks will likely require simple nodes with little computational power, low mobility, potentially large bandwidth but low data rate, and will operate in complicated RF environments. As a result, range-based localization seems most appropriate provided that prevalent non-line-of-sight (NLOS) propagation can be handled. Additionally, synchronization cannot be assumed *a priori* and due to the low complexity requirement, either centralized processing or very simple distributed algorithms will be required.

Due to the potential of 5G and IoT, and the importance of localization in both, we expect a new thrust in research on collaborative localization. It is thus timely to both take stock and look forward. In this paper, we provide an overview of recent progress in collaborative localization. We treat collaborative localization first from an abstract point of view, introducing general models and a brief Fisher information analysis. Then, we specialize in two directions. First, we consider range-based collaborative localization, such as envisioned in a UWB-based IoT, where Fisher information in particular provides insight into the value of both line-of-sight (LOS) and NLOS links. Due to the nonlinear and nonconvex nature of distance measurements, a variety of algorithms will be discussed and evaluated. Second, we consider 5G millimeter-wave (mmWave) collaborative localization, for which the basic measurement model allows estimation of both distances and angles. We perform a Fisher information analyses and propose localization algorithms, at the link and network level.

Notation: Vectors will be denoted with a bold letter (e.g., $\mathbf{x}$) and matrices in bold capitals (e.g., $\mathbf{X}$). When $\mathbf{X}\succcurlyeq 0$, $\mathbf{X}$ is a positive–semidefinite matrix. $\mathrm{tr}\{\mathbf{X}\}$ denotes the trace of $\mathbf{X}$; $[\mathbf{X}]_{n,m}$ is the entry on row n, column m;$[\mathbf{X}]_{n\times n,k}$ is the kth $n \times n$ block diagonal; and $[\mathbf{X}]_{n:m,k:l}$ extracts the submatrix from rows n through m and columns k through l. $\mathbb{E}_{\mathbf{x}}\{\cdot\}$ represents the expectation with respect to $\mathbf{x}$. Finally, $\nabla_{\mathbf{x}}$ is the gradient with respect to $\mathbf{x}$.

II. MODELS AND APPROACH

In this section, we will provide a generic overview of the network localization problem, measurement modalities, fundamental performance bounds, and algorithms. These generic formulations will then be specialized in later sections for range-based and 5G localization.

A. Network Model

We consider a network of A anchor nodes, with known position and/or orientation and N agent nodes with unknown position and/or orientation. We denote the state of node i by $\mathbf{x}_i$, comprising the position $\mathbf{p}_i$ and possibly the orientation. When needed, states of anchor nodes will be denoted by $\mathbf{a}_i$. The nodes are assumed to have perfectly synchronized clocks[2] (unless otherwise noted) and are equipped with one or more radio technology: one technology for measuring distance (range) and possibly a different technology for communication. The nodes are collected into a vertex set $\mathcal{V}$, while links between nodes are collected in an edge set $\mathcal{E} \subseteq \mathcal{V}$. Communication and measurements between nodes are bidirectional, so that $(\mathcal{V}, \mathcal{E})$ forms an undirected graph. The set of neighbors of a node i is denoted by $\mathcal{V}_i$, the set of adjacent anchor nodes of a node i is denoted by $\mathcal{A}_i$, and the set of adjacent agent nodes of a node i is $\mathcal{N}_i$, with $\mathcal{V}_i = \mathcal{A}_i \cup \mathcal{N}_i$. An example of a cooperative network is provided in Fig. 1. In this scenario, agent nodes are not able to estimate

[2]It should be noted that perfect synchronism is assumed in most of this discussion, but is not necessary for time-based ranging. As discussed above, two-way ranging allows for asynchronous ranging.

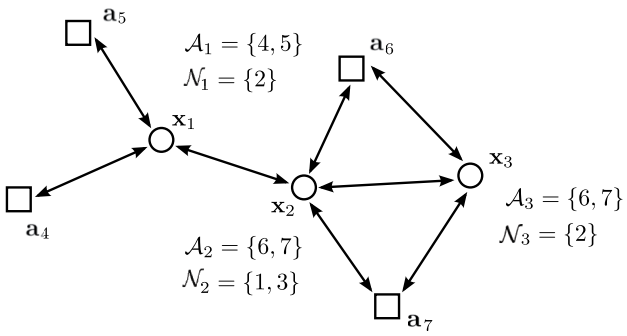

Fig. 1. ***Example of a cooperative network. The squares and circles represent anchor nodes and agent nodes, respectively.***

their locations $\mathbf{p}_1, \mathbf{p}_2, \mathbf{p}_3$ if they rely on only communication with anchor nodes. However, if the agent nodes cooperate with each other, their locations can be determined without ambiguity. The objective of the network is to determine the position and orientation of each agent node, based on measurements $\mathbf{y}_{ij}$ between node pairs $(i,j) \in \mathcal{E}$.

B. Measurement Model

Measurements will be of the form

$$\mathbf{y}_{ij} = \mathbf{f}\left(\mathbf{x}_i, \mathbf{x}_j, \mathbf{b}_{ij}\right) + \mathbf{n}_{ij} \tag{1}$$

where $\mathbf{f}(\cdot)$ is a function dependent on the states of both nodes i and j, $\mathbf{b}_{ij}$ is a nuisance parameter of appropriate dimension, and $\mathbf{n}_{ij}$ is measurement noise. Measurements can take on a variety of forms, based on the available technology and the level of abstraction involved. Generally, three levels of abstraction are considered for modeling.

1) High-level abstraction: measurements are relative states, so that

$$\mathbf{f}\left(\mathbf{x}_i, \mathbf{x}_j, \mathbf{b}_{ij}\right) = \mathbf{x}_i - \mathbf{x}_j + \mathbf{b}_{ij}. \tag{2}$$

This type of measurement assumes the presence of an underlying positioning algorithm for each agent.

2) Medium-level abstraction: measurements are a simple function of the nodes' states. For instance

$$\mathbf{f}\left(\mathbf{x}_i, \mathbf{x}_j, \mathbf{b}_{ij}\right) = \|\mathbf{x}_i - \mathbf{x}_j\| + \beta_{ij} \tag{3}$$

for distance estimation in the presence of an NLOS bias β_{ij}.

3) Low-level abstraction: measurements are at the waveform level. For instance

$$\mathbf{f}\left(\mathbf{x}_i, \mathbf{x}_j, \mathbf{b}_{ij}\right) = p\left\{s\left(t - \left(\|\mathbf{x}_i - \mathbf{x}_j\| + b_{ij}\right)/c\right) + n(t)\right\} \tag{4}$$

in which $\mathbf{f}(\cdot)$ is now the vector expansion of a waveform, $s(t)$ is a transmitted waveform, c is the speed of light, and $p\{\cdot\}$ is an appropriate processing function.

In general, low-level abstractions require more processing, but have the benefit of retaining more information regarding the nodes' states.

C. Fisher Information and the CRLB

The Cramér–Rao lower bound (CRLB) is a useful tool to understand the fundamental behavior of estimation algorithms in general, and localization algorithms in particular. The CRLB is derived from the Fisher information matrix (FIM), which measures the amount of information the observations carry, on average, regarding the unknown parameters [17]. When the FIM of a parameter $\mathbf{z}$, denoted by $\mathbf{J}(\mathbf{z})$, is nonsingular, the CRLB is

$$\mathbf{J}^{-1}(\mathbf{z}) \preccurlyeq \mathbb{E}\left\{(\mathbf{z} - \hat{\mathbf{z}})(\mathbf{z} - \hat{\mathbf{z}})^{\mathrm{T}}\right\} \tag{5}$$

where $\hat{\mathbf{z}}$ represents any unbiased estimator, and the expectation is taken over all possible noise realizations. The CRLB is generally quite loose, especially at low signal-to-noise ratio (SNR), however it still offers an excellent design guideline (at both the link level and the network level) to optimize localization performance. Parameter estimation problems may involve nuisance parameters, which are unknowns not directly related to the state/location of the transmitter or the receiver. A typical example is the clock bias between two devices. For such cases, we apply the concept of the equivalent FIM (EFIM) [18]: given a parameter vector $\mathbf{z} = \left[\mathbf{x}^{\mathrm{T}}, \mathbf{b}^{\mathrm{T}}\right]^{\mathrm{T}}$, where $\mathbf{x}$ relates to the location/state and $\mathbf{b}$ does not, then the FIM can be structured as

$$\mathbf{J}(\mathbf{z}) = \begin{bmatrix} \mathbf{J}(\mathbf{x}) & \mathbf{J}_{\mathbf{xb}} \\ \mathbf{J}_{\mathbf{xb}}^{\mathrm{T}} & \mathbf{J}(\mathbf{b}) \end{bmatrix} \tag{6}$$

where $\mathbf{J}(\mathbf{x})$ is the FIM of the state vector $\mathbf{x}$, $\mathbf{J}(\mathbf{b})$ is the FIM of the nuisance parameters $\mathbf{b}$, and $\mathbf{J}_{\mathbf{xb}}$ represents the information coupling. The EFIM of $\mathbf{x}$, denoted as $\mathbf{J}^{\mathrm{E}}(\mathbf{x})$, is the matrix which contains all of the information necessary to determine the CRLB of $\mathbf{x}$. In other words, if we extract the elements of the inverse of $\mathbf{J}(\mathbf{z})$ which pertain to $\mathbf{x}$ they are equivalent to the inverse of the EFIM of $\mathbf{x}$. The position error bound (PEB) for the kth agent node bounds the square root of the mean square error of position error and is written as

$$\mathrm{PEB}(\mathbf{x}_k) \triangleq \sqrt{\mathrm{tr}\left\{\left[\left(\mathbf{J}(\mathbf{z})\right)^{-1}\right]_{2\times 2,k}\right\}} = \sqrt{\mathrm{tr}\left\{\left(\mathbf{J}^{\mathrm{E}}(\mathbf{x}_k)\right)^{-1}\right\}}. \tag{7}$$

The CRLB can also be used to answer fundamental questions, such as whether collaboration is always beneficial. It can be shown that despite the fact that collaboration introduces new unknowns to be estimated, it will strictly reduce the CRLB of the existing network position estimates under very modest conditions [10]. In particular, for a D-dimensional state, the CRLB is strictly decreasing when a collaborating node is added to a network, provided that this node introduces at least $D + 1$ measurements, one of which must

be related to another agent node. It can also be shown that the collaborating node will also improve its own estimate.

Important insights can also be obtained regarding the use of (collaborative) LOS and NLOS links: LOS links can help to reduce the CRLB and increase the rank of the FIM [11]. NLOS links have unknown biases and do not contribute to the CRLB of position error (assuming that we know which links are LOS and which are NLOS) [19], [20], in the absence of *a priori* information. When *a priori* information on the biases is available, this can improve the FIM [19], [21]. While in practice obtaining knowledge of the distribution is challenging (especially for single shot estimation), having some information on the biases can provide improvement, especially with practical estimators [22]. In the general case of multipath, we are interested in estimating the TOA of the first arriving multipath [23]. The CRLB is available for these situations, although at practical SNR it is found to be unrealistically optimistic leading to the development of other bounds [24], [25].

D. Taxonomy of Algorithms

Algorithms for solving the collaborative localization problem can be categorized in several different ways. However, we believe that the following dichotomies are most helpful in understanding algorithm design: 1) measurement type; 2) centralized versus distributed; 3) sequential versus concurrent; and 4) Bayesian versus one shot. We will discuss each of these descriptions in turn.

1) Measurement Type: Depending on the measurement $\mathbf{y}$ being used, localization algorithms can be classified as distance based [via received signal strength (RSS) or TOA], connectivity based, angle-of-arrival (AOA) based, fingerprinting (RSS is common here), and various hybrid methods. For example, algorithms proposed in [26]–[32] are all connectivity-based approaches. On the other hand, algorithms such as those in [33]–[42] use distance-based localization. Others use various measurements such as WiFi fingerprints, acoustic measurements, magnetic fingerprints, or some fusion of those measurements (e.g., [8] and [43]–[45]). In general, connectivity-based localization has lower device and computational complexity, but results in poorer accuracy. Distance-based localization, on the other hand, leads to more accurate location estimation, but requires range estimation and higher computational complexity. Hybrid approaches utilize multiple measurement types such as distance and angle [46]. Additionally, TOA (which can be based on synchronized nodes, two-way ranging, or time-difference approaches) is more accurate than RSS-based approaches.

In this paper, we focus on approaches which are more applicable to emerging network types such as IoT and 5G cellular. As such, we emphasize range-based approaches using high bandwidth, but low data rate devices (applicable to IoT), and hybrid range-angle-based approaches (applicable to 5G cellular). As discussed previously, we anticipate emerging IoT networks to rely on TOA-based localization while 5G networks will likely exploit both TOA and AOA measurements.

2) Centralized Versus Distributed: Another way to classify localization algorithms is based on where the computation is performed. In centralized approaches [27], [29], [30], [39]–[42], [47]–[53], all the anchor locations and measurement data are forwarded to a central processor to compute the unlocalized nodes' positions in a joint manner. In distributed approaches [6], [28], [34], [36], [38], [54]–[62], the computation is spread over the entire network and thus only local information exchange is required. Distributed approaches have the advantage of being scalable and more robust to node failures. Centralized approaches, on the other hand, utilize information about the entire network and are supposed to yield more accurate location estimation. However, an efficient solver for large-scale nonlinear optimization problems associated with centralized approaches is needed to truly achieve the global optimum. Due to node complexity limitations, IoT applications will be limited to either centralized approaches or distributed approaches which require very limited and simple local processing. 5G cellular on the other hand allows for more processing power in the handset, and thus could support either distributed (calculations in the handsets) or centralized (calculations in the location server) techniques equally well.

3) Sequential Versus Concurrent: Based on how location information is propagated through the network, localization algorithms can also be classified as sequential localization or concurrent localization. In sequential approaches [34], [38], [59], [63], each unlocalized node updates itself as a virtual anchor to assist other unlocalized nodes to localize themselves. In the sequential approaches, only measurements with neighboring nodes are used and thus these approaches tend to be distributed. One drawback of sequential approaches is the propagation of localization error [64], [65], which occurs due to the fact that virtual anchors have localization error and will affect any unlocalized node that uses range estimates to them. On the other hand, in the concurrent approaches, unlocalized nodes do not act as virtual anchors even after they have been localized. Examples include all the centralized approaches and the distributed algorithms proposed in [6], [36], [55], [56], [66], and [67]. Generally speaking, although sequential location estimation appears to be a simple way of disseminating location information throughout the network, the problem of localization error propagation has seriously limited its performance.

4) Bayesian Versus One Shot: Another way to classify existing algorithms is whether the position location problem is formulated in a probabilistic manner. Specifically, depending on the nature of the framework as well as the returned location estimates, existing algorithms can be divided into deterministic and probabilistic approaches. Deterministic approaches assume that the position is a deterministic, but unknown value. Such approaches solve

position location problem in different ways, including the maximum-likelihood approach, optimization-based algorithms [27], [37], [39]–[42], [50], [51], [68], estimation-based methods [48], [69], and other *ad hoc* algorithms, e.g., [26], [28], [34], [36], [55], [56], and [70]. Another approach uses simulated annealing to minimize the sum of the square distance errors [71], [72]. A common feature of these algorithms is that they only compute a deterministic one-shot location estimate for agent nodes. In other words, there is generally no additional information about the quality or the reliability of this solution. Metrics such as distance residual, GDOP, and error ellipses, which do provide some sense of reliability, may not be appropriate for collaborative position location, especially in the presence of NLOS propagation. Further, no distribution information for the nodes' positions is required for these approaches since they are assumed to be deterministic.

On the other hand, in probabilistic localization approaches (or Bayesian approaches) [6], [60]–[62], [73], [74], the position location problem is formulated as a probabilistic inference problem, with the goal of computing (approximating) the probability distribution of each unlocalized node's location. Under such a framework, a position location algorithm can return a set of possible location estimations, each of which is preferably, although not necessarily, associated with a weight quantifying the uncertainty, or equivalently the reliability, about the corresponding location estimate. In this sense, probabilistic approaches return a more direct representation of the solution quality. However, existing algorithms under the probabilistic localization framework often have much higher computational complexity than one-shot algorithms, which can be a limiting factor for low-power sensor deployment. However, low-complexity versions have been investigated as well (e.g., [75]).

5) One-Shot Estimation Versus Tracking: The majority of the approaches discussed above are one-shot estimators (i.e., non-Bayesian) which do not exploit historical data or motion models. Classic tracking, however, exploits motion models and the series of measurements when nodes are mobile to improve estimation. Such approaches are generally Bayesian approaches. The only difference between tracking algorithms and the Bayesian approaches discussed above is that tracking assumes node mobility and incorporates the mobility model into the *a posteriori* probability. Examples of such approaches in collaborative localization include [6], [42], and [76]–[79].

III. RANGE-BASED WIDEBAND LOCALIZATION

IoT-type networks will likely rely on simple radios and require relatively low data rates. A prime candidate for the physical layer of such networks (when there is need for localization) is UWB or spread spectrum signals combined with range-based TOA measurements. Additionally, due to the limited processing capabilities of IoT devices, we focus on centralized algorithms or distributed algorithms which require very limited local processing. Finally, we address the primary practical issues in collaborative localization when applied to IoT: multipath/NLOS propagation, the need for noise variance knowledge, and node synchronization.

A. Measurement Model

Range-based wideband (e.g., UWB) localization is typically studied using one of two basic models. A low-level abstraction model uses a waveform model where the received signal between nodes i and j can be written as

$$y_{ij}(t) = \sum_{l=0}^{L-1} h_{ij}^{l} s\left(t - \epsilon_{ij}(t) - \left(\|\mathbf{x}_i - \mathbf{x}_j\| + b_{ij}^{l}\right)/c\right) + n_{ij}(t) \quad (8)$$

where $s(t)$ is the time-domain waveform (typically with large bandwidth to allow accurate timing measurements), h_{ij}^{l} is the complex channel coefficient for the lth multipath component (of L total received components), $\epsilon_{ij}(t)$ is the synchronization error due to clock skew and offset (initially assumed to be zero), b_{ij}^{l} is a positive bias due to NLOS propagation (i.e., the additional distance traveled by the signal due to reflections), and $n_{ij}(t)$ is zero-mean Gaussian noise whose variance is directly related to the SNR of the link.

A second model commonly used in range-based collaborative localization uses a medium level of abstraction and directly models the measured distances (ranges) d_{ij} between any two nodes i and j

$$d_{ij} = \|\mathbf{x}_i - \mathbf{x}_j\| + \beta_{ij} + v_{ij} \quad (9)$$

where β_{ij} is the resulting NLOS-induced distance estimation bias[3] and v_{ij} is Gaussian error due to AWGN.

B. Localization Algorithms

Now that we have examined the collaborative localization problem from an information point of view, we will focus on algorithms to perform the estimation. Consider a set of N agent nodes located in an area L, whose locations are represented by a vector $\mathbf{x} \in \Re^{2\times N}, \mathbf{x} \in \mathcal{L}^{N}$. The problem at hand is to find an estimate of the location/state of agent node $\mathbf{x}$ given a series of noisy measurements $\mathbf{y}$. We will start with the assumption that $\mathbf{x}$ is a deterministic, but unknown value.

1) Maximum Likelihood: Maximum-likelihood (ML) estimation is a popular method of estimating unknown parameters of a statistical model. The ML estimator has several attractive limiting properties (when the number of measurements tends to infinity). The ML estimator is asymptotically optimal, meaning that as the number of measurements increases, its accuracy can reach the CRLB.

[3]Note that b_{ij}^{l} are the biases associated with each multipath while β_{ij} is the resulting bias in the estimated range. If there were only a single resolvable multipath component, then $\beta_{ij} = b_{ij}^{1}$.

It is also asymptotically normal, meaning that as the measurement size increases, the distribution of the ML estimator approaches a Gaussian distribution with mean of $\mathbf{x}$ (asymptotically unbiased) and a covariance matrix equal to the inverse of the FIM. Finally, the ML estimator is consistent, meaning that as the number of measurements increases, the ML estimator converges to the true parameter.

The ML estimator is obtained by maximizing the likelihood function of the measurement model [17]. Assuming Gaussian noise corrupts $\mathbf{y}$, the ML solution can be shown to be equal to a weighted least squares solution

$$\hat{\mathbf{x}} = \arg\min_{\mathbf{x}} \sum_{i=1}^{N} \left\{ \sum_{j\in\mathcal{A}_i} \frac{1}{\sigma_{ij}^2} \left(y_{ij} - ||\mathbf{x}_i - \mathbf{x}_j||\right)^2 + \sum_{k\in\mathcal{N}_i} \frac{1}{\sigma_{ik}^2} \left(y_{ik} - ||\mathbf{x}_i - \mathbf{x}_k||\right)^2 \right\}. \tag{10}$$

Note that this is a nonlinear, nonconvex optimization problem and does not have a closed-form solution. One method of solving this minimization problem is to use gradient descent which can be done either using a centralized or distributed approach [6]. However, for a gradient descent approach to find the true global minimum, an appropriate starting point is required. Otherwise a local minimum is reached which may be far from the true solution. Similarly, iterative optimization algorithms such as the Gauss–Newton (GN) algorithm can be applied. The GN algorithm also requires an initial point which can be difficult to find and requires some preprocessing time. Moreover, since the cost function of the ML estimation is nonlinear and nonconvex, the GN algorithm may converge to a local minimum or saddle point which causes a large estimation error. Therefore, if the initial point of the Gauss–Newton method is not sufficiently close to the global minimum, it is highly probable that the algorithm converges to a stationary point which is not the global minimum.

The global minimum can be reached using a branch-and-bound (BB) solution search strategy, coupled with the reformulation linearization technique (RLT) [80]. However, this can be highly complex which leads to a desire to find suboptimal methods such as convex optimization using convex approximations of the original objective function. Other slightly less complex approaches (e.g., stochastic search techniques [81]) which can find the global optimum with high probability have also been developed.

2) Semidefinite Programming: Convex relaxation can provide an alternative solution for the convergence problem of the ML estimator. In this technique, the nonlinear and nonconvex ML problem is relaxed into a nonlinear but convex optimization problem. Although such problems are solved iteratively, the solver always converges to the global minimum, no matter how the initial point is selected. Although there are several types of convex optimization problems such as quadratic programming (QP) and second-order cone programming (SOCP), semidefinite programming (SDP) is the most general form of them which can be solved effectively in polynomial time. Since SDP is more general, it allows for wider applications and provides more freedom in relaxation. To apply SDP, we first note that the problem in (10) can be written as an optimization problem [7], [37]

$$\underset{\mathbf{X},\mathbf{Z},t_{ij},t_{kj},d_{ij},d_{kj}}{\text{minimize}} \quad \sum_{i=1}^{N} \left\{ \sum_{j\in\mathcal{A}_i} \frac{t_{ij}}{\sigma_{ij}^2} + \sum_{k\in\mathcal{N}_i} \frac{t_{ik}}{\sigma_{ik}^2} \right\} \tag{11}$$

$$s.t.: \quad t_{ij} = h_{ij} - 2y_{ij}d_{ij} \tag{12}$$

$$h_{ij} = z_{jj} + \mathbf{a}_i^{\mathrm{T}}\mathbf{a}_i - \mathbf{a}_i^{\mathrm{T}}\mathbf{x}_j - \mathbf{x}_j^{\mathrm{T}}\mathbf{a}_i \tag{13}$$

$$h_{ij} = d_{ij}^2, \qquad j \in \mathcal{A}_i \tag{14}$$

$$t_{ik} = h_{ik} - 2y_{ik}d_{ik} \tag{15}$$

$$h_{ik} = z_{ii} + z_{kk} - z_{ik} - z_{ki} \tag{16}$$

$$h_{ik} = d_{ik}^2, \qquad k \in \mathcal{N}_i \tag{17}$$

$$\mathbf{Z} = \mathbf{X}^{\mathrm{T}}\mathbf{X} \tag{18}$$

where $\mathbf{Z}_{ik} = \mathbf{x}_i^{\mathrm{T}}\mathbf{x}_k$. The problem can be relaxed into a faster (albeit less accurate) SDP problem by changing specific equality constraints into inequalities [7], [37]

$$h_{ij} \geq d_{ij}^2 \tag{19}$$

$$h_{ik} \geq d_{ik}^2 \tag{20}$$

$$\mathbf{Z} \succcurlyeq \mathbf{X}^{\mathrm{T}}\mathbf{X}. \tag{21}$$

In this relaxation, rather than finding the solution that is as close as possible to the intersection of the neighboring ranging circles, the solution is allowed to lie anywhere inside the area intersected by those ranging circles. Similar relaxations have been explored using a slightly modified version of the objective function (e.g., minimizing $|y_{ij}^2 - ||\mathbf{x}_i - \mathbf{x}_j||^2|$) resulting in an SOCP [50], [57]. In most cases, the solution from SDP methods is accurate enough and comparable with the optimal solution. However, if the accuracy is not sufficient, the solution of the SDP method can be used as an initial point of GN method to achieve better performance. An additional advantage of this approach is that it can naturally take advantage of NLOS links. The CRLB analysis shows that NLOS links are not useful when there is no information available, but potentially useful even with partial information. The key information used here is that NLOS biases are inherently positive, and typically overshadow errors due to noise.

3) Parallel Projection: The above approaches, as described, are centralized approaches, although distributed versions are possible. However, the structure of the CRLB demonstrates that localization accuracy is dominated by

local information. While centralized approaches seem likely for IoT networks, distributed solutions with very low complexity requirements could be used. A third approach to solving the problem, which is inherently distributed and has low complexity, is the modified parallel projection method (PPM) [7], [66], [67]. In particular, the approach uses the modified PPM as a basic element and extends it to an iterative and distributed numerical framework [66], [82]. The overall framework involves an initialization step and an iterative update step, where only local communications are necessary in both steps. Like the SDP approach, the IPPM takes natural advantage of the fact that NLOS biases are inherently positive, and thus can utilize NLOS links.

In the initialization step, each unlocalized node obtains an initial solution for its location. The approach we adopt is called closest anchor initialization. Specifically, if an unlocalized node has connecting anchor(s), it will use the mean location of its connected anchors $\mathbb{E}\{\mathcal{A}_i\}$, as its initial solution. If an unlocalized node does not have a connection to any anchors, it will use the average location of its surrounding nodes' initial solution as its initial solution. For isolated nodes without any connections, we simply use the network center as the initial solution and due to the absence of range estimates, their estimates will thus not be updated in the ensuing iterative update step. The initialization step continues until every unlocalized node obtains an initial solution. We emphasize that there exist other methods to obtain initial solutions [36], including using the solution from multidimensional scaling (MDS) as an initial solution, but those generally involve substantially more computation. Instead, we use the simple initialization method described above.

In the iterative update step, each unlocalized node uses modified PPM to update its location estimate, based on its range estimates to neighboring nodes $\mathcal{V}_i$, either anchors $\mathcal{A}_i$ or other unlocalized nodes $\mathcal{N}_i$, and its current location estimate. In particular, if the ith and jth nodes are neighbors, the projection of $\hat{\mathbf{x}}_i$ onto the feasibility set given by the range estimate y_{ij} is

$$P_{ij}^{\text{col}}(\hat{\mathbf{x}}_i) = \hat{\mathbf{x}}_j + y_{ij}\frac{\hat{\mathbf{x}}_i - \hat{\mathbf{x}}_j}{||\hat{\mathbf{x}}_i - \hat{\mathbf{x}}_j||}. \tag{22}$$

Since only local information exchange is needed, the iterative update process can be distributed and the computational complexity scales linearly with network size. The new location estimate is then the average of the $|\mathcal{V}_i|$ projections (i.e., one per neighbor). Each unlocalized node examines whether its residual changes over the previous iteration. The ith unlocalized node's residual based on its and its neighbors' current estimated locations is

$$\mathbf{\Phi}^{\text{col}}(\hat{\mathbf{x}}_i) = \frac{1}{|\mathcal{V}_i|}\sum_{j\in\mathcal{V}_i}\left(y_{ij} - ||\hat{\mathbf{x}}_i - \hat{\mathbf{x}}_j||\right)^2 \tag{23}$$

where $\mathcal{V}_i = \mathcal{A}_i \cup \mathcal{N}_i$ is the set of the ith node's neighboring nodes, and $|\cdot|$ denotes cardinality. If its residual has not changed more than the precision parameter δ for κ consecutive iterations, the ith node will quit the iterative update step and mark itself as localized. The overall update process terminates after all of the unlocalized nodes have been marked as localized. Iterative PPM for collaborative position location is described in Algorithm 1.

Algorithm 1: Iterative PPM for Collaborative Position Location

Data: $\mathbf{y}$ measurement vector, $\mathbf{a}$ anchor locations
Result: $\hat{\mathbf{x}}$ agent node location estimate
Initialization:
Obtain initial guess $\hat{\mathbf{x}}_0 = [\hat{\mathbf{x}}_1, \hat{\mathbf{x}}_2, \ldots, \hat{\mathbf{x}}_N]$ using the mean connected anchor initialization; Set $\hat{\mathbf{x}} = \mathbf{a}$ for all anchors, which will remain unchanged during the Main loop.
Set $l = 0$, δ as a small positive number, and κ as a positive integer;
Let $F_i = 0$ and $W_i = 0$, for $i = 1, 2, \ldots, N$;
$\Phi_{i,l} = \Phi^{\text{col}}(\hat{\mathbf{x}}_i)$, for $i = 1, 2, \ldots, N$;
Main Loop:
while *any of* F_i *is equal to 0* **do**
  for i=1,2,...,N **do**
    if $F_i = 0$ **then**
      $\hat{\mathbf{x}}_i \leftarrow (1/|\mathcal{V}_i|)\sum_{j\in\mathcal{N}_i} P_{ij}^{\text{col}}(\hat{\mathbf{x}}_i)$
      $\Phi_{i,l+1} \leftarrow \Phi^{\text{col}}(\hat{\mathbf{x}}_i)$
      if $|\Phi_{i,l} - \Phi_{i,l+1}| < \delta$ **then**
        $W_i \leftarrow W_i + 1$;
        if $W_i \geq \kappa$ **then**
          $F_i \leftarrow 1$
      else
        $W_i \leftarrow 0$
  $l = l + 1$

In Algorithm 1, F_i indicates whether the ith node has been localized and W_i records the number of consecutive iterations that the ith node's residual has not decreased more than δ. Once $W_i \geq \kappa$, we set $F_i = 1$ and consider the ith unlocalized node as localized. It is obvious that anchor location "estimates" are equivalent to the true locations and will remain unchanged during the process. It should be noted that like many iterative algorithms, the final solution of iterative PPM depends on the initial guess.

Compared to the case of noncollaborative position location, we can easily see that the major difference here is that we use $\mathbf{W}_i$ as a means of accumulating observations over multiple iterations regarding whether an unlocalized node is indeed localized. This is understandable since during the iterative update process, if an unlocalized node has updated its location, its neighboring unlocalized nodes may be affected in terms of their residuals, and therefore need to be reexamined. Another advantage of iterative PPM is that the computational load involved is low, mainly because of the simple operation involved in updating node locations which scales linearly with n.

4) Message Passing Approaches: The approaches discussed above are inherently one-shot approaches which treat the position (or state) values to be estimated as deterministic, but unknown values. An alternative approach is to treat the state/position values as random values. Such approaches

are known as Bayesian approaches. These approaches are most naturally applied to mobile agent nodes. We will discuss tracking approaches shortly, although these approaches could rightly be categorized as tracking.

The two most common Bayesian estimators are the minimum mean square error (MMSE) estimator and the maximum *a posteriori* (MAP) estimator. Both estimators depend on the *a posteriori* distribution $p_{\mathbf{x}|\mathbf{y}}(\mathbf{x}|\mathbf{y})$. Specifically, the MMSE estimator uses the mean of the *a posteriori* distribution whereas the MAP estimator uses the mode. Assuming that node movement is 1) independent from node to node and 2) memoryless, the *a posteriori* distribution can be factored. Specifically, if we represent the position vector from $t = 0{:}T$ as $\mathbf{x}^{(0:T)}$ we can perform the following factorization:

$$p(\mathbf{x}^{(0:T)}) = \prod_{t=1}^{T}\prod_{i=1}^{N} p\left(x_i^{(t)} | x_i^{(t-1)}\right). \tag{24}$$

The result is that we can find $p\left(\mathbf{x}^{(t)} | \mathbf{y}^{(1:t)}\right)$

$$p\left(\mathbf{x}^{(t)} | \mathbf{y}^{(1:t)}\right) \propto p\left(\mathbf{y}^{(t)} | \mathbf{x}^{(t)}\right) \int p\left(\mathbf{x}^{(t)} | \mathbf{x}^{(t-1)}\right) p\left(\mathbf{x}^{(t-1)} | \mathbf{y}^{(1:t-1)}\right) \mathrm{d}\,\mathbf{x}^{(t-1)}. \tag{25}$$

The marginalization of (25) can be efficiently accomplished by appropriately factoring (25), creating a factor graph using that factorization and applying the sum product algorithm [6]. This message passing approach can be naturally implemented as a distributed algorithm. Although we have examined Bayesian approaches in the context of mobile nodes, Bayesian approaches have also been applied to stationary node localization [75], [83]–[85].

C. Tracking Algorithms

Another problem which has not gained enough attention in the literature is node tracking in cooperative networks. The difference between static localization (i.e., one shot) and tracking is that in the latter agent nodes are mobile and an underlying dynamic model is used to localize agent nodes over time. In tracking algorithms, since the agent node is mobile, velocity and sometimes acceleration of the agent nodes are estimated along with the location. Few studies have focused on node tracking in NLOS environments [42], [86], [87]. One technique to deal with NLOS propagation is to estimate and track NLOS biases [88]. In this technique (also called bias tracking), all measurements are assumed to be NLOS, including a large positive bias. For each link, an unknown parameter is added to the state vector and estimated jointly with the location and velocity of the agent node. We will later show that the performance of this technique is not as good as expected in many NLOS situations. Moreover, the complexity of the algorithm intensifies as the number of measurements increases, since for each measurement we need to track an unknown bias. Further, the complexity increases exponentially for cooperative localization.

Modeling NLOS/LOS time dependencies using a Markov chain has also been proposed in the literature [86], [87]. The interacting multiple model (IMM) algorithm is used to consider the underlying Markov chain. The major problem with IMM algorithms is that 2^m filters need to be run simultaneously for m measurements and hence the number of required filters grows exponentially with the number of measurements [87]. In [86], Hammes and Zoubir introduce an approximation to decrease the number of required filters. However, the proposed IMM algorithm still needs to know the transition probabilities of the LOS and NLOS states. The performance of the IMM algorithm is highly dependent on the transition probabilities which are very difficult to determine in practice. Using robust estimators which are very popular for static localization [89] provides another solution for node tracking in NLOS propagation [90]. Unlike classic estimators, robust estimators are typically less vulnerable to outliers and NLOS biases. The main advantage of robust estimators is that they typically require no information about the NLOS propagation. In [91], a NLOS mitigation technique based on SDP for cooperative networks is introduced. It is shown that tracking NLOS biases is not a good option. Therefore, to mitigate NLOS propagation, the proposed estimator estimates the NLOS biases jointly with the location and velocity of the agent node. However, the estimator does not track the biases and instead estimates them independently at each time step. Although the complexity of the estimator increases because of the bias estimation, its complexity is lower than estimators which include the biases in the state vector and track them. The proposed estimator is classified as a robust estimator and requires no statistical knowledge about the NLOS propagation.

One important consideration with tracking algorithms is the scheduling of measurements during node movement. Specifically, it is important to minimize the number of measurements while maintaining a specific localization accuracy. In [92], Wang *et al.* develop a framework for evaluating scheduling strategies for measurements and propose a situation-aware scheduling approach to mitigate the evolution of network localization error. Further, a computational geometry approach is developed in [93] which allows for evaluation of various node prioritization strategies to balance localization error and network resource consumption. This can be useful in both localization and tracking algorithm development.

D. Impairments and Practical Considerations

1) Unknown Noise Variance: In the derivation of the localization algorithms in Section III-B, we have assumed that the variance of measurement noise for each connection is known. However, in many networks, the noise variance is not available or difficult to determine. This problem can be handled in multiple ways. One can simply use the same variance for all the links $\left(\text{e.g., } \sigma_{ij}^2 = 1\right)$, although the accuracy

of the algorithms would be lower than the case where the variance of measurements is provided. Another way to deal with this problem is to use the inverse of measured ranges as the variance of measurement noise $\left(\text{i.e., } \sigma_{ij}^2 = 1/y_{ij}^2\right)$. This is due to the fact that the accuracy of the range measurement is dependent on the SNR of the signal at the receiver, which itself is a function of the distance between the transmitter and the receiver. Therefore, larger measured ranges tend to have larger noise variance.

2) NLOS Propagation: There are four levels of knowledge concerning NLOS propagation: a) no knowledge of which links have NLOS biases nor any knowledge of the bias distributions; b) knowledge of the NLOS links (i.e., identification), but no knowledge of the bias distributions; c) knowledge of the distributions and identification; and d) full knowledge of the NLOS biases.

The first case is typically handled using robust estimation approaches. One such example is the IPPM method described above [7], [67]. Such robust estimators do not make any attempt to distinguish between LOS and NLOS connections, but instead rely on the overall approach to be robust to NLOS biases. A similar approach is described in [40] which formulates the cooperative positioning problem as an implicitly convex feasibility problem. Like the previously mentioned techniques, it assumes neither the identification of NLOS links nor the NLOS distribution. Both techniques rely on the fact that NLOS biases are typically larger than Gaussian measurement noise. As a result, the measurement error is generally positive allowing the problem to be formulated as convex sets. Essentially, the algorithm exploits the NLOS errors and thus is reasonably robust to them. In [41] again, no knowledge of NLOS is assumed (neither identification nor distributions). Instead all links are assumed to be biased [using the measurement model of (4)] and the presumed bias on each link is estimated as part of minimizing the square error between the observations and the measurement model. The nonlinear set of equations is relaxed to form an SDP with a feasibility region defined by the positive biases. To account for the fact that some links are in fact LOS and thus may have negative errors, the constraints are loosened requiring $||\mathbf{x}_i - \mathbf{x}_j||^2 \leq y_{ij}^2 + 2\sqrt{\text{var}(y_{ij})}$ where $\text{var}(y_{ij})$ is the estimated variance of the range measurements.

The second case requires identification of NLOS links, which can be done using various statistics, particularly delay spread [94]–[97]. When armed with NLOS identification, one approach to handling NLOS propagation is to discard NLOS measurements as suggested by the CRLB [98]. However, this is problematic when there are an insufficient number of LOS links (a common situation in indoor environments). Additionally, it has been shown when dealing with practical algorithms that NLOS links can be used to improve performance. As an example, one approach uses LOS links to create the objective function and the NLOS links to create the feasible region in a linear program (LP) [98]. However, this approach requires at least three LOS connections. This can be handled by converting NLOS links to virtual LOS links through range scaling [59]. Similarly, the approach of [22] relies on identification of NLOS links to separate measurements to be used in the objective function versus those to be used in defining constraints in an SDP.

When the distribution of NLOS biases is known (in addition to identifying NLOS links), various approaches can be used in an attempt to utilize this additional information. One approach is to estimate the biases along with the position parameters. However, this is typically an underdetermined problem leading to estimation difficulties. However, if estimation can be accomplished, performance can potentially be substantially improved. An alternative is to incorporate the bias values into the Gaussian measurement noise. For example, assuming an exponentially distributed bias, the algorithm of [39] approximated the measurement noise as a Gaussian random variable with a mean value equal to the mean of the bias distribution and a variance that is the sum of the variance of the bias and measurement noise. Using this approximation, the ML objective function was formulated and relaxed into an SDP. As a second example, the work in [99] developed an ML approach based on the product of range likelihoods when the channel statistics are known. In the same vein, the algorithm in [75] is a message-passing approach which assumes that the ranging error is distributed according to an asymmetric double exponential. The approach exploits this NLOS knowledge efficiently, but obviously requires the parameters of the double exponential to either be known (e.g., through propagation surveys) or somehow estimated online.

It should be noted that several models for the TOA bias due to NLOS propagation have been proposed. As discussed in various places (e.g., see [75], [89], [99], and [100]) ranging error in the presence of NLOS bias is usually modeled as a shifted or mixed Gaussian distribution, where the shift or second distribution is used to model the NLOS bias and the Gaussian is used to model the error due to noise. When mixture models are used, the bias distribution is modeled using a uniform distribution, an exponential distribution, or a Rayleigh distribution [89], [100]. Additionally, a skew-t distribution has recently been proposed to model NLOS error [101] as well as the double-exponential model [75].

3) Multipath Proagation: As mentioned earlier, in addition to scenarios where no LOS path exists, there are scenarios of interest where the LOS may exist, but is corrupted by multipath. In this situation, range estimation requires determination of the delay associated with the first arriving path. The optimal detector for this case (with *a priori* knowledge of the channel statistics) is evaluated in [25]. The ML estimator for Orthogonal frequency division multiplexing-type waveforms was presented and evaluated in [23]. A practical

threshold-based estimator for UWB signals was developed in [102]. It was found that the proposed estimator is biased unless the threshold is chosen to be substantially larger than the noise. Further, it was shown that if the first arriving path suffers from fading, the probability of identifying the first arriving path dominates the TOA estimation error. In general, the bias due to multipath propagation can be treated in a manner similar to the bias due to NLOS propagation.

4) Synchronization: Range-based localization using TOA can either be done using synchronized clocks or asynchronous clocks. The latter requires two-way ranging as discussed earlier. Synchronism between agent nodes may not be necessary for TOA-based ranging (and thus localization), however, it may be desirable for other reasons. Although it may be reasonable to assume that the anchor nodes' clocks are synchronized with each other, it is typically not reasonable to assume that the agent nodes are synchronized with each other or with the anchor nodes. The lack of synchronization among nodes in a network is mainly due to their different clock parameters (i.e., clock skew and offset). Since sensors have different hardware implementations, each sensor has its own specific clock. Moreover, the clocks inside sensors are highly sensitive and their parameters may change over time.

In wireless networks, clock synchronization is typically performed by transferring a series of time stamp messages among the nodes, called TOA measurements. Moreover, the accuracy of clock synchronization impacts the localization performance in the network. Small differences between the clocks at the nodes may lead to significant localization errors. The reason is that the location of an agent node is estimated from a series of time stamps which are a function of the agent node clock parameters. If exact information about the clock parameters is not available, the measured time stamps will deviate from their true values leading to significant errors in location estimation. Typically in asynchronous networks, the clocks at the nodes are first synchronized and then localization is performed. However, this approach can lead to poor synchronization performance which dramatically impacts localization accuracy [103]. Recently, several studies have focused on joint synchronization and localization in a wireless network, as there is a close relationship between the two and they can be performed simultaneously. It has been shown that joint synchronization and localization can provide significant improvements over the two-step approach [103], [104]. This is mainly due to the fact that in the two-step approach, each link between an agent node and an anchor node is treated independently, while in the joint approach the relationship between multiple links (which is the location of the agent node) is used in the estimation.

The internal clocks of the nodes are assumed to be imperfect, a trait which causes the internal time to drift away from the reference time and thus $\epsilon_{ij}(t) \neq 0$. The relationship between the internal time of the ith agent node and the reference time is modeled as [104]–[106]

$$t_i = \omega_i t + \theta_i \tag{26}$$

where t_i and t are the internal time of the ith node and the reference time, respectively, ω_i is the clock skew, and θ_i represents the clock offset. The lack of synchronization at node may be attributed to the fact that each node has a unique clock, meaning that the clock skew and offset are different for each node.

Consider a slave node k at coordinates $\mathbf{x}_k \in \mathbb{R}^2$ and a master node i at coordinates $\mathbf{x}_i \in \mathbb{R}^2$. The slave node refers to the node that initiates the transmission and wants to synchronize its own clock with that of the master node. There are two common clock synchronization techniques in WSNs: one-way message dissemination and two-way message exchanges [105]. In the one-way message dissemination technique, either the slave node or the master node transmits the synchronization messages, while in the two-way technique, both slave and master nodes transmit the synchronization messages. Several rounds of the messages are usually transferred between the nodes to achieve higher accuracy. At the mth round of transmission, the slave node k transmits the forward signal at time stamp T_{kim} and master node i receives the signal at time stamp R_{kim}. Master node i then sends back a signal at $\overline{T}_{ikm}$ and slave node k captures the backward signal at $\overline{R}_{ikm}$. Time stamps T_{kim} and $\overline{R}_{ikm}$ are reported based on the internal clock of node k, while R_{kim} and $\overline{T}_{ikm}$ are reported based on the internal clock of node i. The measured time stamps at the receivers are modeled as [104]

$$\begin{aligned} R_{kim} &= \frac{\omega_i}{\omega_k} T_{kim} + \omega_i (t_{ki} + n_{kim}) - \frac{\omega_i}{\omega_k} \theta_k + \theta_i \\ \overline{R}_{ikm} &= \frac{\omega_k}{\omega_i} \overline{T}_{ikm} + \omega_k (t_{ik} + \overline{n}_{ikm}) - \frac{\omega_k}{\omega_i} \theta_i + \theta_k \end{aligned} \tag{27}$$

where $t_{ki} = t_{ik}$ is the propagation time between nodes k and i, given by $t_{ki} = 1/c \, \| \mathrm{x}_k - \mathrm{x}_i \|$. The terms n_{kim} and $\overline{n}_{ikm}$ represent the measurement errors which are modeled as independent and identically distributed (i.i.d.) Gaussian random variables. As can be seen from (27), for localization purposes, the clock parameters of agent nodes are considered as nuisance parameters. This means that the clock parameters are unknown and have to be estimated along agent locations, but their estimates are not of immediate interest. As mentioned earlier, a common approach is to estimate the clock parameters first and remove their impact from the measurements. In this way, the measured ranges among nodes can be obtained and any localization algorithm discussed in Section III-C can be used to localize the agent nodes. Another way to deal with asynchronous networks is to jointly estimate the clock parameters and agent locations directly from the measured time stamps using semidefinite programming techniques as described in [104].

It has been shown in [104] that the latter case provides better localization performance than the former case. An additional approach recently proposed is to perform joint localization and synchronization using message passing approaches [107].

E. Results

To provide insight into the performance of collaborative localization under various levels of NLOS knowledge, the following example is provided. A network with ten anchor nodes and 30 agent nodes is considered and nodes are randomly distributed in an area of 25 m by 25 m with 30% and 70% of the connections being LOS and NLOS, respectively. The range measurement noise is drawn from a Gaussian random variable and its variance is assumed to be proportional to distance $\sigma^2 \propto d^\beta$ where $\beta = 2$ for LOS and $\beta = 4$ for NLOS. The NLOS biases are drawn from an exponential random variable with a random mean uniformly distributed from 0 to 15 m.

Fig. 2 shows the connectivity as a function of communication range for 100 network realizations. As communication range of nodes increases, connectivity in the network increases. For instance, at 30-m communication range, the connectivity is 100%, meaning that all nodes are connected to each other. At 15-m communication range, the connectivity is 60%, meaning that the nodes on average are connected to 60% of other nodes.

One of the main advantages of collaborative localization is the improvement in node localizability. Node localizability refers to a situation in which the location of an agent node can be determined uniquely and without any ambiguity (i.e., the FIM is invertible). For a 2-D noncooperative network, each agent node must be connected to at least three noncollinear anchor nodes to be localizable. This criterion leads to the need for a high anchor node density in the network to ensure all agent nodes are connected to enough anchor nodes (i.e., the FIM without collaborative links is invertible). On the other hand, in a 2-D cooperative network, an agent node needs to have at least three disjoint paths to noncollinear anchor nodes. The path can be established through intermediate agent nodes and unlike noncooperative networks a direct path to an anchor node is not required. Fig. 2 also shows the cumulative distribution function (CDF) of localizability versus number of collaborators and communication range. In the noncooperative case, agent nodes are only connected to anchor nodes within their communication range. For the cooperative cases, the agent nodes are connected to both anchor nodes and other agent nodes within their communication range. In the case where there are more neighboring agent nodes than the desired number of collaborators, agent nodes select their collaborators randomly from among their neighbors. Since multiple random network realizations are examined, the impact of choosing specific neighbors is captured in the overall statistics. It can be seen from Fig. 2 that collaboration among nodes can significantly improve node localizability in the network at a given communication range (i.e., the addition of collaborative links leads to an invertible FIM). Agent nodes in cooperative networks require shorter communication ranges and equivalently lower power consumption to be localizable. Significant improvement is achieved by one or two collaborators, but the rate of improvement slows down as the number of collaborators goes beyond two. For instance, if in a network the communication range is only 8 m due to power and interference limitations, only 45% of the agent nodes are localizable without cooperation. Localizability improves by 25% to 70% if each agent node communicates with only one other agent node. Localizability further improves by an additional 10% to 80% if each agent node communicates with two other agent nodes.

Fig. 3 shows the CDF of the CRLB of agent node locations for 100 network realizations under different NLOS situations. The communication range is fixed at 20 m to

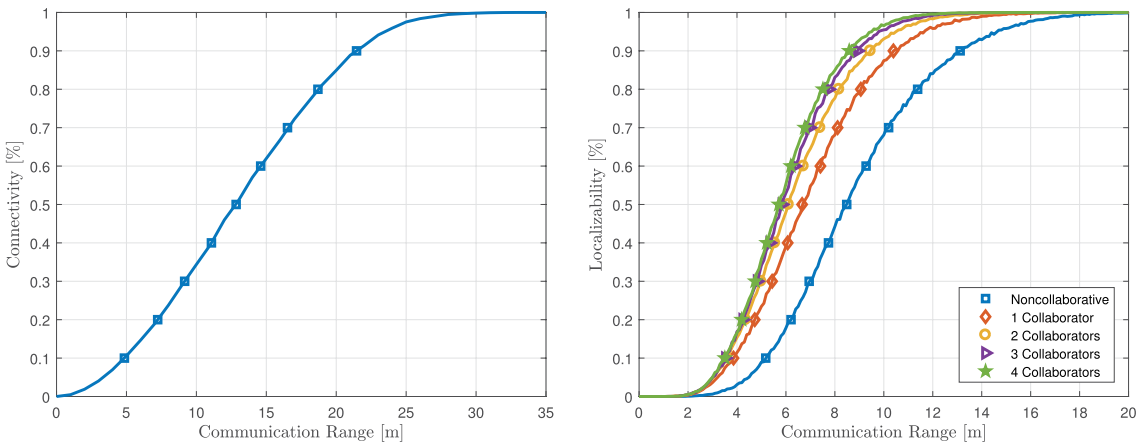

Fig. 2. ***Network connectivity (left) and node localizability (right) as a function of communication range.***

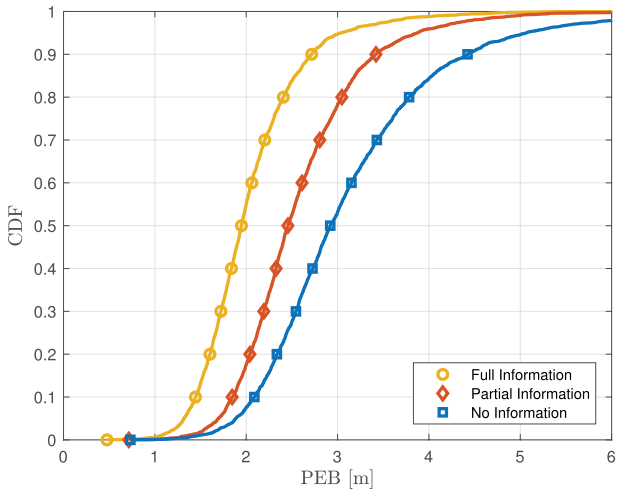

Fig. 3. ***Example CRLBs with full information, partial information, and no information about NLOS biases.***

ensure all nodes are localizable. Fig. 3 shows that the CRLB (PEB) with full NLOS information provides an absolute lower bound on the localization performance. On the other hand, when there is no information about NLOS biases except for NLOS ID, the performance is limited by the curve marked with blue squares. In general, the lack of information increases the lower bound on the error by over 50%. Finally, the CRLB with partial information (i.e., having statistical knowledge of NLOS bias) falls roughly halfway between the two previous cases which shows that having some information about NLOS links can be beneficial.

In Fig. 4, two specific localization techniques are compared to see if this trend is consistent with actual estimators, viz., nonlinear least squares (NLLS) and SDP. The NLLS method solves the nonlinear problem in (10). In this simulation, the NLLS problem is solved by the MATLAB routine lsqnonlin which uses the Levenberg–Marquardt algorithm. The algorithm is initialized with true values to increase the chance of convergence to the global minimum, although in practice various initialization approaches have been used. Additional detail concerning the robust SDP method is provided in [41]. Note that there are two plots. Fig. 4(a) shows the performance when the noise variance is assumed known, while Fig. 4(b) shows the performance when the noise variance is unknown and assumed to be the same on each link. NLLS with full information about NLOS propagation and noise variance provides the optimal performance. In this case, the estimator knows which connections are NLOS[4] and their NLOS biases are available. Therefore, NLOS biases are removed from the measurements and the problem in (10) is solved including all measurements. Further, when noise variance information is available, links are weighted according to the inverse of the noise variance, allowing less reliable links to have less impact on the solution. NLLS with no NLOS information provides the worst performance, as the algorithm naively uses the measurements without taking the NLOS biases into consideration. NLLS with partial information falls between these two cases demonstrating the benefit of having some information about NLOS propagation. In this case, the estimator knows which connections are NLOS, however, no information about the distribution of NLOS biases is available. Therefore, the NLOS connections are neglected and the problem in (10) is solved using only LOS measurements. The robust SDP method designed for an NLOS environment performs better than naive NLLS and is lower bounded by NLLS with partial

[4]This, of course, requires NLOS identification. A number of research efforts have examined means for distinguishing between LOS and NLOS connections (e.g., [94], [95], and [108]).

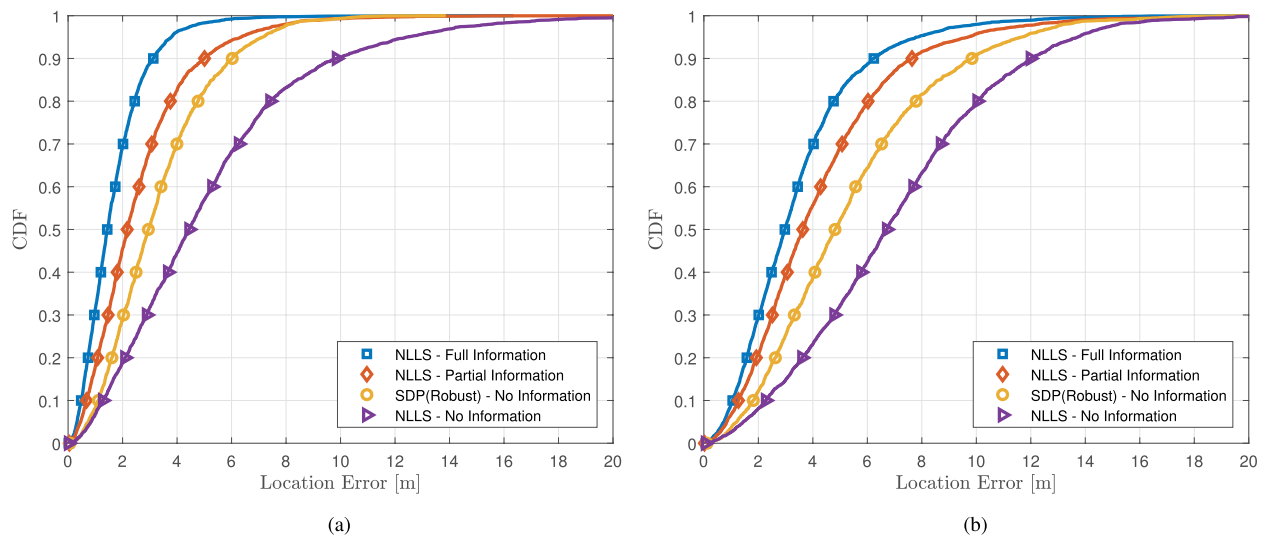

Fig. 4. ***CDF of location error for different localization techniques. The NLLS method solves the nonlinear problem in (10). (a) Known noise variance. (b) Unknown noise variance.***

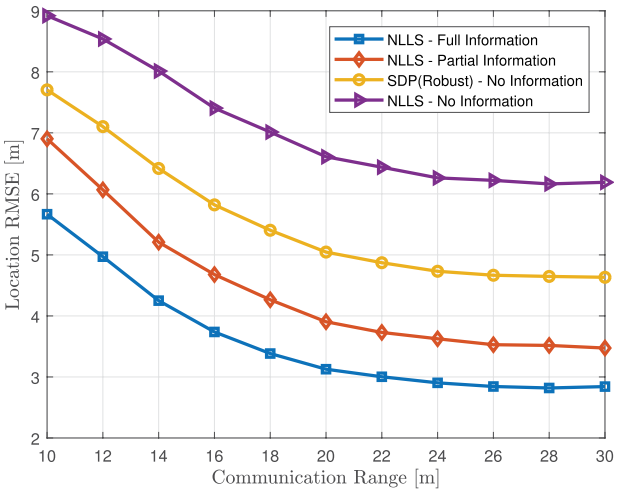

Fig. 5. ***Location RMSE versus communication range. The NLLS method solves the nonlinear problem in (10).***

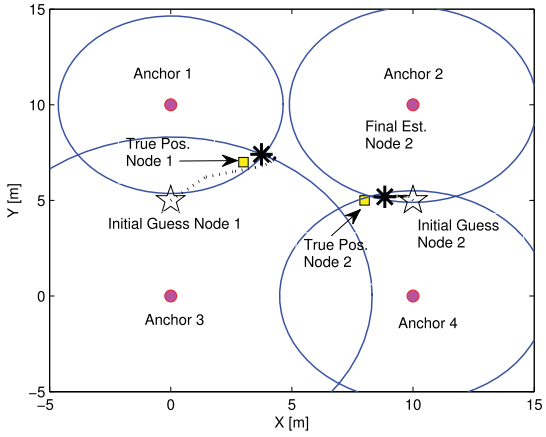

Fig. 6. ***Example performance of IPPM. Note that squares denote the true node positions, the stars represent the initial guesses, and the asterisks represent the final solution. Circles represent the range information.***

information, as the estimator does not have any information regarding NLOS biases.[5] We can also see that information concerning the noise variance is just as important (perhaps slightly more important) in cooperative localization as the error increases between 50% and 100% when all links are treated equally, regardless of the bias information available.

Fig. 5 shows the localization root mean square error (RMSE) versus communication range for the four localization algorithms discussed in Fig. 4. Localization performance improves as communication range among nodes increases. This is mainly due to the fact that by increasing communication range in the network, more measurements will be available for each agent node. Fig. 5 also shows that the improvement rate is significant by increasing the communication range from 10 to 20 m, while the improvement rate decreases as communication range increases beyond 20 m. This can be easily explained from Fig. 2 which shows that the network connectivity improves significantly by going from a communication range of 10 to 20 m. However, increasing communication range from 20 to 30 m does not significantly improve connectivity.

An example of the performance of IPPM is given in Fig. 6. In this example, two agent nodes are located at $\mathbf{x}_1 = [3,7]^{\mathrm{T}}$ and $\mathbf{x}_2 = [8,5]^{\mathrm{T}}$. Node 1 can communicate with anchors 1 and 3 (denoted by the two ranging circles to the left) while node 2 can communicate with anchors 2 and 4 (denoted by the two ranging circles to the right). Thus, neither node can unambiguously localize itself without collaboration. However, by communicating with each other, localization is possible. An initial position estimate is chosen based on the mean of the anchor locations with which it is connected. The dotted lines represent the IPPM iteration whereas the asterisks represent the final estimates. At each iteration, a node must exchange its current estimate of its location, but location estimates are calculated locally (i.e., in a distributed fashion). The final estimates are well within 1 m of the true locations with an RMSE of 0.85 m. Note that 1) this case required ten iterations to obtain the final result; and 2) in this case, the solution is nearly identical (within 5 mm) to the ML solution.

In Fig. 7, we compare the algorithms discussed in Section III-C as well as three additional algorithms in the presence of NLOS propagation using the same parameters as described above. The solution of ML method uses only the LOS links and is provided with two different initial values. ML-True and ML-Anchor curves represent the performance of the ML algorithm when the solver is initialized with the true values of agent locations and the average of anchor node locations, respectively. As expected, ML-True provides the best performance (although it does not exploit known noise

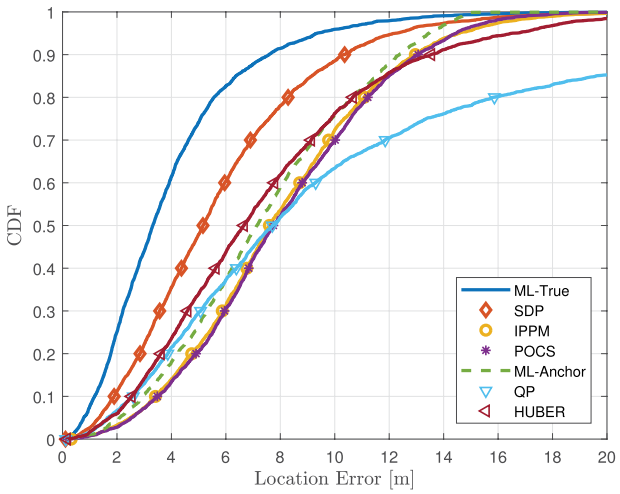

Fig. 7. ***CDF of location error for the algorithms in Section III-C.***

[5]It should be noted that although the SDP algorithm does not have explicit information about the NLOS biases, it does exploit the knowledge that NLOS biases are typically larger than Gaussian noise errors.

variance which would improve it even further). However, as can be seen, the ML method requires a proper initialization to ensure that the algorithm converges to the global minimum. In practice this is hard to guarantee. The SDP method provides slightly worse performance as compared to ML-True, but given that the algorithm does not require any initialization and has significantly lower computational complexity it is a very promising approach. ML-Anchor performs worse than SDP, showing the importance of initial values on the performance of the ML method. IPPM performs slightly worse than ML-Anchor, but it has much lower complexity and can be implemented in a distributed manner. Note that the IPPM method is also initialized with the average location of anchor nodes. However, our simulations (not shown here) reveal that the performance of IPPM is less sensitive to the initial solution than the ML method.

Three other localization algorithms are also included in Fig. 7 for comparison: a nonlinear estimator based on the Huber function in [109], a projection onto convex sets (POCS) method described in [110], and a quadratic programming (QP) method in [111]. In the Huber algorithm, a piecewise cost function is used to mitigate NLOS propagation. In this way, the cost function will have different weights for each measurement based on the absolute value of residual error. POCS is an iterative and distributed approach which requires simple computations and generally shows strong robustness against NLOS propagation. This algorithm starts with an initial solution and updates the solution by projecting the location estimate onto the circles formed by measurements (similar to IPPM). In the QP algorithm, the locations of agent nodes are estimated using an optimization approach with quadratic constraints such that the final estimate of an agent node must fall within the circles defined by its range measurements. It tends to be more susceptible to NLOS propagation as seen in the figure. Although the approach has similarities to SDP, we see that the performance is much worse, showing the importance of properly handling constraints and the relaxation approach. Note that both IPPM and POCS are simple and distributed approaches which are based on projecting the solution on the circles defined by range measurements. However, in each iteration, the former updates the solution by averaging over all the projections, while the latter updates the solution using only one projection. Thus, the results are fairly similar. These distributed approaches perform worse than the centralized SDP approach, but are still better than QP and similar to Huber both of which are also centralized. Thus, being centralized or distributed is not as important to algorithm performance as how the algorithm handles NLOS measurements.

IV. RANGE- AND ANGLE-BASED 5G LOCALIZATION

In the context of 5G communications, collaborative localization is expected to play an important role, as 5G will support D2D communication through so-called sidelinks, which may be controlled by a base station. Communication in uplink, downlink, and sidelink can take place over two distinct frequency bands: below 6 GHz and above 24 GHz. While there have been activities in the sub-6-GHz band [112], the latter so-called mmWave band is interesting for localization [113], [114], due to the large available bandwidth, sparse propagation channel, and the presence of large antenna arrays at both transmitter and receiver [115]. These properties allow for increased angle and especially delay resolution, compared to conventional multiantenna localization [46], [116], which mainly relied on subspace-based methods such as MUSIC or ESPRIT. In mmWave, the use of directional beamforming, the constraints imposed by hybrid arrays, the possibility of D2D connectivity, and the availability of efficient channel estimation methods based on compressed sensing call for novel collaborative localization methods, based on insights from fundamental performance analysis. In this section, we describe the mmWave localization model, derive the FIM, and overview algorithms for localization and tracking, in both collaborative and noncollaborative settings.

A. Link-Level Measurement Model

In mmWave communication, the high carrier frequency and smaller wavelengths lead to a reduced energy capture at the receiver antenna. To compensate for this effect, large antenna arrays are used together with precoding at the transmitter and combining at the receiver. The observation model for a link between two devices can be expressed in an OFDM format, for a total bandwidth $1/T_s$, divided into N_s subcarriers [117]

$$\mathbf{y}[n] = \mathbf{W}^{\mathrm{H}}[n] \sum_{l=0}^{L-1} h_l \mathbf{a}_r(\theta_l)\mathbf{a}_t^{\mathrm{H}}(\phi_l)\mathbf{F}[n]\boldsymbol{s}[n]e^{-j2\pi\tau_l n/(N_s T_s)} + \mathbf{W}[n]^{\mathrm{H}}\mathbf{v}[n] \tag{28}$$

where, for the lth propagation path ($l = 0,\ldots,L-1$), we have complex gain $h_l = \rho_l e^{j\psi_l}$, $0 < \rho_l \in \mathbb{R}$, path delay (TOA) τ_l, AOA θ_l and angle-of-departure (AOD) ϕ_l, with corresponding response vectors $\mathbf{a}_r(\theta_l)$ and $\mathbf{a}_t(\phi_l)$. The AOA is measured with respect to the local reference frame of the receiver, while the AOD is measured with respect to the local reference frame of the transmitter. The matrices $\mathbf{W}[n] = \mathbf{W}_{\mathrm{RF}}\mathbf{W}_{\mathrm{BB}}[n]$ and $\mathbf{F}[n] = \mathbf{F}_{\mathrm{RF}}\mathbf{F}_{\mathrm{BB}}[n]$ are combining and precoding matrices for subcarrier n, respectively. Here, the number of columns of the RF matrices $\mathbf{W}_{\mathrm{RF}}$ and $\mathbf{F}_{\mathrm{RF}}$ will be denoted by M_r and M_t, respectively, and represent the number of RF chains at the receiver and the transmitter. Hence, the matrices $\mathbf{W}[n]$ and $\mathbf{F}[n]$ can be used for directional transmission and allow for reduced RF hardware complexity at transmitter and receiver [115] when $M_t \ll N_t$ and $M_r \ll N_r$. The number of columns of the baseband precoding matrix $\mathbf{F}_{\mathrm{BB}}[n]$ is no greater than M_t and represents the number of supported streams on subcarrier n. We

assume $\mathbf{W}[n]$ to have orthogonal columns (possibly after suitable whitening) so that $\mathbf{W}[n]^{\mathrm{H}}\mathbf{W}[n] = \mathbf{I}_{M_r}$ and $\mathbf{F}[n]$ is such that $\|\mathbf{F}[n]\|_{\mathrm{F}}^2 = 1$. The vector $\mathbf{s}[n] \in \mathbb{C}^{M_t}$ comprises the transmitted symbols on subcarrier n, with $\mathbb{E}\{\mathbf{s}[n]\mathbf{s}^{\mathrm{H}}[n]\} = E_s\mathbf{I}_{M_t}$, and $\mathbf{v}[n] \sim \mathcal{CN}(0, N_0\mathbf{I}_{N_r})$ is additive noise, independent across subcarriers.

B. Geometric Relationships

In order for the above model to be useful for localization, we tie the channel parameters to the geometry of the propagation environment [46], [118]. This is possible, due to the lack of shadowing and diffraction, and the limited number of propagation paths in the mmWave communication channel [119]. Limiting ourselves to a 2-D scenario with point scatterers, we will denote the locations of the transmitter, the receiver, and the lth scatterer by $\mathbf{x}_t = [x_t, y_t]^{\mathrm{T}}$, $\mathbf{x}_r = [x_r, y_r]^{\mathrm{T}}$, and $\mathbf{s}_l = [x_l, y_l]^{\mathrm{T}}$, respectively, while the orientations of the transmitter and the receiver are α_t and α_r, respectively. All locations and orientations are measured with respect to an absolute frame of reference, as depicted in Fig. 8. From the figure, it follows immediately that for the LOS link (designated as path 0, though it does not need to be present) $\tau_0 = \|\mathbf{x}_t - \mathbf{x}_r\|/c$, $\phi_0 = \mathrm{atan}(y_r - y_t)/(x_r - x_t) - \alpha_t$, and $\theta_0 = \phi_0 + \pi - \alpha_r$. For the other multipath components (numbered by $l > 0$), $\tau_l = \|\mathbf{x}_t - \mathbf{s}_l\|/c + \|\mathbf{s}_l - \mathbf{x}_r\|/c$, $\phi_l = \mathrm{atan}(y_l - y_t)/(x_l - x_t) - \alpha_t$, and $\theta_l = \mathrm{atan}(y_r - y_l)/(x_r - x_l) + \pi - \alpha_r$. From these geometric relations, it becomes apparent that in the mmWave regime, when the parameters of the paths can be resolved, both the location and orientation of an agent can be determined by exchanging signals with a single anchor. Finally, under the considered scatterer model, each path provides information regarding the incidence points $\mathbf{s}_l$, which allows the receiver to sense the environment. These statements will be confirmed through a Fisher information analysis in Section IV-C.

Remark 1: The relationships between the channel parameters and the environment rely on a geometric, spatially consistent channel model, e.g., the map-based model from [120].

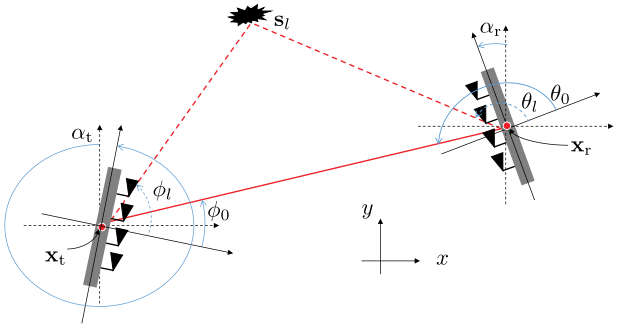

Fig. 8. ***Geometric relations between the transmitter and receiver locations, as well as possible scatterers, relative to an absolute coordinate (shown as x and y). All angles are measured counterclockwise.***

We have ignored effects of diffuse scattering, AOA and AOD spread [121], as well as the impact of the illumination angle and reception angle of the precoding and combining matrices on the effective channel. Such effects require further study, in order to obtain realistic, yet tractable mmWave channel models for positioning and mapping. Such models may be different from those used for communication. We note that other parameterizations of the channel parameters are also possible [119], [122]. Reflecting surfaces can be associated with so-called virtual anchors,[6] corresponding to the locations of the transmitter mirrored with respect to the surfaces. Virtual anchors have the benefit that their locations do not depend on where the receiver is, while incidence points do. For convenience, we treat the incidence points as scatterers with fixed locations in 2-D space.

C. FIM Analysis

Before we can study the network FIM, we must gain understanding regarding the single-link FIM. This latter FIM captures how well we can estimate the receiver's location and orientation, in the frame of reference of the transmitter, based on the observation model (28). It also reveals the impact of the scatters and the precoding matrix. We will then turn to the network FIM, which tells how information is diffused within the network and how orientation uncertainty affects position uncertainty.

1) Single-Link FIM: For a single link, we will operate in the frame of reference of the transmitter, so that we can set $\mathbf{x}_t = [0, 0]^{\mathrm{T}}$ and $\alpha_t = 0$. We will start from the noise-free observation, take derivatives with respect to the unknown parameters, $\mathbf{z} = [\mathbf{x}_r^{\mathrm{T}}, \alpha_r, \mathbf{s}_1^{\mathrm{T}}, \ldots, \mathbf{s}_{L-1}^{\mathrm{T}}]^{\mathrm{T}}$, and then compute an outer product to obtain the FIM. The noise-free observation is given by

$$\mathbf{f}[n] = \mathbf{W}^{\mathrm{H}}[n] \sum_{l=0}^{L-1} \rho_l e^{j\psi_l} \mathbf{a}_r(\theta_l)\mathbf{a}_t^{\mathrm{H}}(\phi_l)\mathbf{F}[n]\mathbf{s}[n] e^{-j2\pi\tau_l \frac{n}{N_s T_s}}. \tag{29}$$

Taking the gradient $\nabla_{\mathbf{z}}\mathbf{f}[n]$ and computing the outer product, the FIM can be determined as [17]

$$\mathbf{J}(\mathbf{z}) = \frac{2}{N_0} \sum_{n=0}^{N_s-1} \Re\left\{\nabla_{\mathbf{z}}^{\mathrm{H}}\mathbf{f}[n] \nabla_{\mathbf{z}}\mathbf{f}[n]\right\} \tag{30}$$

as each subcarrier provides independent information. From this FIM, we can directly obtain the PEB as

$$\mathrm{PEB}(\mathbf{z}) = \left(\mathrm{tr}\left[\mathbf{J}^{-1}(\mathbf{z})\right]_{1:2,1:2}\right)^{1/2}. \tag{31}$$

In addition to the PEB, we can also determine the so-called orientation error bound (OEB) as $\mathrm{OEB}(\mathbf{z}) = \left[\mathbf{J}^{-1}(\mathbf{z})\right]_{3,3}^{1/2}$ and the scatterer position error bound (SCPEB) as

$$\mathrm{SCPEB}(\mathbf{z}) = \frac{1}{\sqrt{L-1}}\left(\mathrm{tr}\left[\mathbf{J}^{-1}(\mathbf{z})\right]_{4:2(L+1),4:2(L+1)}\right)^{1/2}. \tag{32}$$

[6]Note that the term "virtual anchor" here differs from the one used in Section II-D3, where it referred to a well-localized agent.

The FIM is generally well conditioned (provided $N_s \times M_r \geq 4L + 1$) but does have an obvious structure to be exploited. A detailed analysis of this type of Fisher information can be found in [123] and [124], which showed that antenna arrays provide position Fisher information in two orthogonal directions.To gain insight into the fundamental localization behavior, we consider a system with $N_s = 16$ subcarriers, uniform linear arrays with $N_r = N_t = 32$ antennas with half-wavelength spacing, quadrature phase shift keying (QPSK) training data, a 30-GHz carrier and 100-MHz bandwidth. The SNR is set to be approximately 5 dB at 10 m under full multiple-input–multiple-output (MIMO) transmission (i.e., when $M_t = N_t$ and $\mathbf{F}[n] = \mathbf{I}_{N_t}$ and $\mathbf{W}[n] = \mathbf{I}_{N_r}$). Paths are generated according to a geometric model with random phase and gain proportional to the path loss (determined by the distance of each path, with a path loss exponent 2). We set $\mathbf{W}[n] = \mathbf{I}_{N_r}$ and $\mathbf{F}[n] = \mathbf{F}$, comprising $M_t \in \{3, 32\}$ columns from a scaled DFT matrix. The environment comprises five scatterers. In Fig. 9, a map of the PEB across a 2-D space for $M_t = 3$ is shown. Beams are pointed toward $\{0, \pm 0.0625\}$ rad, though the individual beams are not visible. The area illuminated by the beams is clearly noticeable and has a low PEB. Outside the main lobes of the beams, the PEB rapidly increases to large values. This indicates that beamforming is beneficial, provided the receiver is in the main lobe of the beams. The 99% confidence ellipses in the beams show that information is mainly obtained from the AOA and AOD, less from the delay. The OEB (not shown) exhibits similar behavior.

For further quantitative results, we turn to Fig. 10, showing the fraction of the area that is able to achieve a certain PEB. This can be interpreted as a CDF of the PEB over the deployment area. Under beamforming with $M_t = 3$ beams,

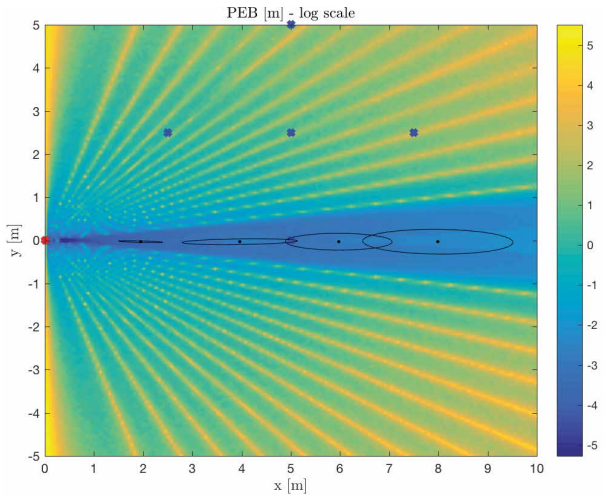

Fig. 9. ***PEB(z) across space for a scenario with three beams and five scatterers (marked in blue) with 99% confidence ellipses (enlarged five times) are shown for four locations. Note that a PEB values of [10 m, 1 m, 10 cm, 1 cm] correspond to value of [+2.3, 0, −2.3, −4.6] in the log domain.***

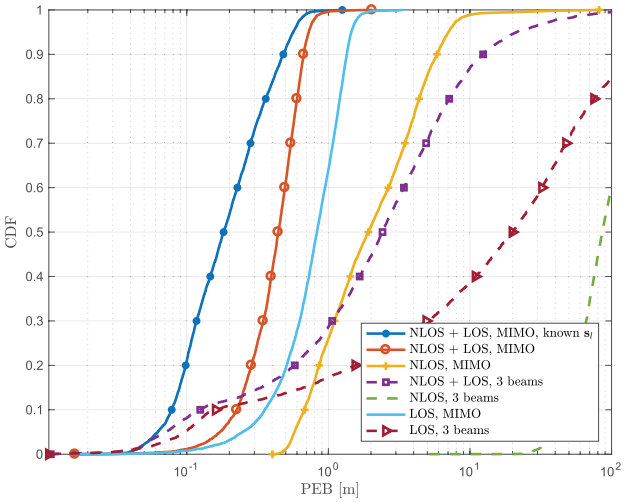

Fig. 10. ***PEB coverage under different operating conditions: LOS only, LOS with five paths, and NLOS only. For each, the performance under MIMO and $M_t = 3$ beamforming is shown.***

we see that under LOS (i.e., only a LOS path is present) and LOS+NLOS (i.e., both LOS and five NLOS paths are present) conditions, a low PEB (below 20 cm) is achieved for a small fraction of the area, corresponding to the area illuminated by the beams. The NLOS paths are beneficial in reducing the PEB, even though the scatterer locations are unknown. When the LOS path is not available, the PEB is large across the deployment area. Under MIMO transmission ($M_t = 32$), the situation improves for most of the deployment area, except for those 10% of locations that benefited from the $M_t = 3$ beams. This shows a tradeoff between accuracy and coverage, adjustable by the transmit beamforming. Interestingly, even when the LOS path is absent, around 30% of the deployment area can achieve a PEB of less than 1 m. As in the beamforming case, LOS+NLOS (six paths) is better than LOS only (one path[7]), though both achieve submeter accuracy for nearly 100% of the deployment area. When the locations of the scatterers are known *a priori*, the PEB further improves significantly, with 60% of the deployment area having a PEB of less than 20 cm, mainly in the vicinity of the scatterers. Fig. 11 shows the performance in terms of the SCPEB, i.e., how well the scatterers can be localized. Under beamforming, the performance is poor, as only one of the scatterers is illuminated by the beams. Under MIMO, with NLOS+LOS, the SCPEB is close to the PEB (a coverage PEB of 90% for 0.67 m and an SCPEB coverage of 90% for 1.1 m), meaning that it is possible to localize the scatters. *A priori* knowledge of the receiver's location and orientation (i.e., known $\mathbf{x}_r, \alpha_r$) turns out to provide some gains in terms of the SCPEB. While we have not shown results for the OEB, they are similar to the PEB

[7]We have modeled each path as an additional source of power. When the total power is fixed and spread out over paths, the NLOS cases would have worse performance.

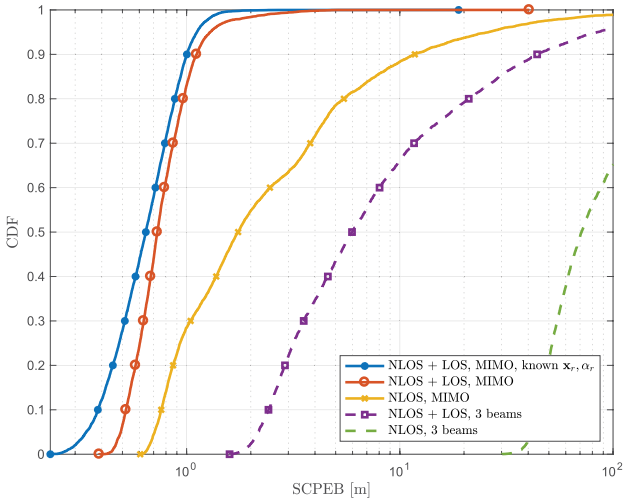

Fig. 11. ***SCPEB coverage under different operating conditions: LOS with five paths, and NLOS only. For each, the performance under MIMO and $M_t = 3$ beamforming is shown. Note the different scale compared to Fig. 10.***

results, though in this case the scatterers do not add much information in addition to the LOS path.

From the above discussion, we see that single-link localization in 5G mmWave has several interesting properties.

- Single-anchor localization: In contrast to range-based localization, where a single anchor provides only 1-D Fisher information, 5G signals from a single anchor provide a full-rank FIM. Hence, single-anchor localization becomes possible [125], providing estimates of $\mathbf{x}_r$ and α_r, in the frame of reference of the transmitter. This ability was already noted in [46] in the context of conventional MIMO, though without accounting for beamforming.
- Sensing: The ability to estimate both distances and angles provides the opportunity to directly estimate scatterers and virtual anchors [119], [126]. This information can be used to map the environment, which in turn aids in the positioning of other nodes [127], [128].
- NLOS localization: In addition to the ability to localize with a single anchor, 5G mmWave localization also allows determining a position in the absence of a LOS path. When there are $L-1$ scatterers, corresponding to $2(L-1)+3$ unknowns (including the position and orientation of the receiver), the estimation of $3(L-1)$ time, AOD, and AOA parameters can give a nonsingular FIM, when $L \geq 3$ [126].
- Uplink versus downlink: The above formulation considered the transmitter to have a known location and orientation. When the transmitter has an unknown location and orientation, the roles of AOA and AOD reverse. This leads to an asymmetry in uplink and downlink, as AOA information is often larger than AOD information, thus providing a benefit for uplink localization in which the receiver's location is known [129].

2) FIM for Collaborative Localization: From the above analysis, we conclude that from a single link between nodes i and j, we obtain an estimate of a) the relative location $\mathbf{x}_j - \mathbf{x}_i$; and b) the relative orientation $\alpha_j - \alpha_i$. This is in contrast to range-based localization, where the link-level estimate is related to the internode distance $\|\mathbf{x}_i - \mathbf{x}_i\|$, as in (9). This in turn changes the FIM for network localization [11]. We express the estimate at node i with respect to node j as

$$\mathbf{y}_{ij} = \underbrace{\left[\left[\mathbf{R}_{\alpha_i}\left(\mathbf{x}_j - \mathbf{x}_i\right)\right]^{\mathrm{T}}, \left(\alpha_j - \alpha_i\right)\right]^{\mathrm{T}}}_{\doteq \mathbf{m}_{ij}\left(\mathbf{x}_i, \mathbf{x}_j, \alpha_i, \alpha_j\right)} + \mathbf{n}_{ij} \tag{33}$$

where $\mathbf{n}_{ij} \sim \mathcal{N}(\mathbf{0}, \Sigma_{ij})$ is estimation noise. We have introduced a rotation matrix $\mathbf{R}_{\alpha_i} = [\cos\alpha_i \ \sin\alpha_i; \ -\sin\alpha_i \ \cos\alpha_i]$. In other words, node i measures the relative orientation of its neighbor j, and the relative position of j in the frame of reference of node i. When node i is an anchor, we set $\mathbf{R}_{\alpha_i} = \mathbf{I}_2$, assuming all anchors have the same orientation. Considering a scenario with $\Sigma_{ij} = \Sigma = \mathrm{diag}\left(\Sigma_p, \sigma_o^2\right)$, where Σ_p is a 2×2 position estimation error covariance matrix, σ_o^2 is the orientation error variance, and with two measurements per link (i.e., $\mathbf{y}_{ij}$ in the frame of reference of node i and $\mathbf{y}_{ji}$ in the frame of reference of node j), the network FIM for a network with N agents is a $3N \times 3N$ matrix[8] with diagonal block matrices denoted by $\mathbf{J}_{ii}$ and off-diagonal block matrices denoted by $\mathbf{J}_{ij}$, derived from

$$\nabla_{[\mathbf{x}_i^{\mathrm{T}}, \alpha_i]^{\mathrm{T}}} \mathbf{m}_{ij}(\mathbf{x}_i, \mathbf{x}_j, \alpha_i, \alpha_j) = \begin{bmatrix} -\mathbf{R}_{\alpha_i} & \dot{\mathbf{R}}_{\alpha_i}(\mathbf{x}_j - \mathbf{x}_i) \\ \mathbf{0}^{\mathrm{T}} & -1 \end{bmatrix} \tag{34}$$

and $\nabla_{[\mathbf{x}_i^{\mathrm{T}}, \alpha_i]^{\mathrm{T}}} \mathbf{m}_{ji}(\mathbf{x}_i, \mathbf{x}_j, \alpha_i, \alpha_j) = \mathrm{diag}(\mathbf{R}_{\alpha_j}, 1)$. Introducing $\dot{\mathbf{R}}_{\alpha_i} = \partial \mathbf{R}_{\alpha_i} / \partial \alpha_i$, the transformed noise covariance $\mathbf{Q}_i = \mathbf{R}_{\alpha_i}^{\mathrm{T}} \Sigma_p^{-1} \mathbf{R}_{\alpha_i}$, $\dot{\mathbf{Q}}_i = \mathbf{R}_{\alpha_i}^{\mathrm{T}} \Sigma_p^{-1} \dot{\mathbf{R}}_{\alpha_i}$, $\ddot{\mathbf{Q}}_i = \dot{\mathbf{R}}_{\alpha_i}^{\mathrm{T}} \Sigma_p^{-1} \dot{\mathbf{R}}_{\alpha_i}$, and $\bar{\Delta}_i = \sum_{j \in \mathcal{V}_i} (\mathbf{x}_j - \mathbf{x}_i)$, we find that

$$\mathbf{J}_{ii} = \begin{bmatrix} |\mathcal{V}_i| \mathbf{Q}_i + \sum_{j \in \mathcal{V}_i} \mathbf{Q}_j & -\dot{\mathbf{Q}}_i \bar{\Delta}_i \\ -\bar{\Delta}_i^{\mathrm{T}} \dot{\mathbf{Q}}_i^{\mathrm{T}} & \sum_{j \in \mathcal{V}_i} \|\mathbf{x}_j - \mathbf{x}_i\|_{\ddot{\mathbf{Q}}_i}^2 + 2|\mathcal{V}_i| / \sigma_o^2 \end{bmatrix} \tag{35}$$

where $\|\mathbf{x}\|_{\mathrm{A}}^2 = \mathbf{x}^{\mathrm{T}} \mathbf{A} \mathbf{x}$. We observe that the fact that the orientation is unknown introduces the off-diagonal entries in (35), which creates a coupling between location information and orientation information. We also see that from the position-related part of the measurement, additional information regarding the rotation is obtained (i.e., the terms $\|\mathbf{x}_j - \mathbf{x}_i\|_{\ddot{\mathbf{Q}}_i}^2$). Finally, the FIM lacks symmetry in i and j, as the measurements themselves are not symmetric.

[8]The mixed scenario where some nodes are position anchors and some are orientation anchors can be derived similarly.

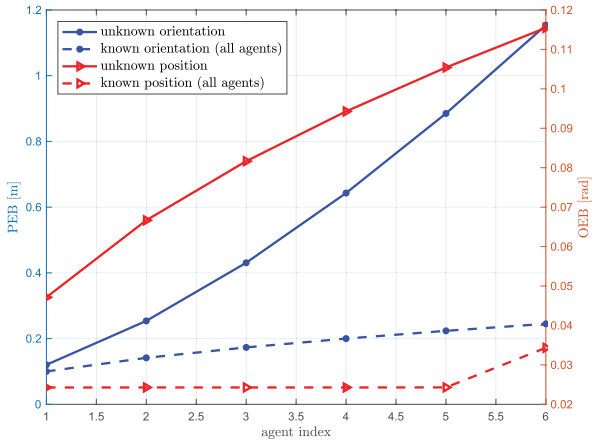

Fig. 12. ***Network PEB and OEB for a line network with one anchor and ten agents. The PEB increase of the due to unknown orientations occurs mainly in the lateral direction (i.e., orthogonal to the direction between the nodes).***

For two agents with $(i, j) \in \mathcal{E}$

$$\mathbf{J}_{ij} = \begin{bmatrix} -\mathbf{Q}_i - \mathbf{Q}_j & -\dot{\mathbf{Q}}_j(\mathbf{x}_j - \mathbf{x}_i) \\ -(\mathbf{x}_j - \mathbf{x}_i)^{\mathrm{T}}\dot{\mathbf{Q}}_i^{\mathrm{T}} & -2/\sigma_o^2 \end{bmatrix}. \tag{36}$$

Fig. 12 shows the PEB and OEB, derived from the inverse of the FIM, for a linear network with one anchor and ten agents, each node located at $\mathbf{x}_i = [2i, 2i]^{\mathrm{T}}$ with $\alpha_i = 0$, $\sigma_o = 0.2$ rad, $\Sigma_p = \mathrm{diag}(0.01\,\mathrm{m}^2, 0.01\,\mathrm{m}^2)$. As expected, the PEB and OEB increase the farther away the agent is from the anchor. The impact of the coupling between position and orientation is revealed in the dashed curves: the PEB when the agent orientations are known is significantly smaller and grows significantly slower than when the agent orientations are unknown. Similar findings hold for the OEB. In particular, when the locations of the agents are known, the OEB depends only on the number of connected nodes, not on their rotation uncertainty. Fig. 13 shows the location uncertainty ellipses, derived from $\mathbf{J}^{-1}$. We observe that the faster than linear increase in the uncertainty when the orientations are unknown is solely in the lateral direction.

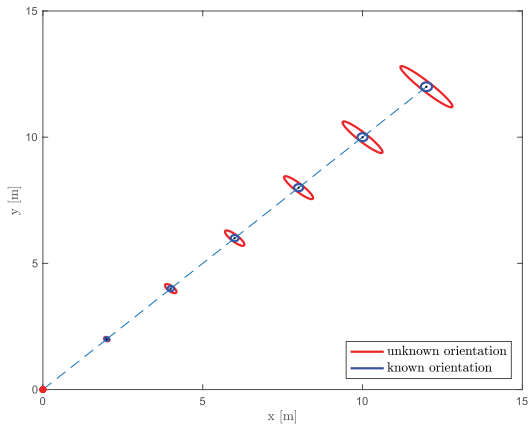

Fig. 13. ***Uncertainty ellipses (one sigma) derived from $\mathbf{J}^{-1}$. The uncertainty increase due to unknown orientations occurs in the lateral irection (i.e., orthogonal to the line between the nodes).***

Remark 2: Collaboration was only used for estimation of the position and orientation of the devices, not of the scatterers. The network FIM can include scatterers, when the observations are the received OFDM signals between nodes. This FIM computation is difficult due to an inherent data association problem (i.e., which scatterer corresponds to which path between nodes). It was shown in [130] that for sufficiently high SNR and nonoverlapping scatterers, the FIM tends to the FIM under perfect data association, which can be obtained similarly to (30).

D. Localization

In this section, we explore options for determining the locations and orientations of the agents. As in previous sections, we first consider a single link, for which we aim to obtain the relative location and orientation of a receiver, in the frame of reference of the transmitter. Then, we move on to a complete network, where we may have *a priori* knowledge of the position and orientation of some nodes. In both cases, we will work in a Bayesian setting, providing not only point estimates, but also uncertainty information. For the 5G network localization problem, it is preferred to have distributed solutions, spreading out the communication and computing burden over the network, rather than collecting and processing all measurement at single entity.

1) Link Level: We consider again the case where the transmitter has a known location and orientation. In order to estimate the receiver's location and orientation, we can resort to either direct positioning or indirect (or two-stage) positioning. Direct positioning has the benefit of leading to better performance, though at an increased computational cost [131], [132]. Two-stage positioning involves first estimating angles and delays from the observed waveform, and then the position and orientation from these estimated angles and delays. Two-stage positioning leads to information loss, but is computationally less demanding and can reuse standard channel estimation routines, already present in the receiver. Since the channel can be described with few parameters (complex gains, AOAs, AODs, and delays), parametric channel estimation [133] has performance and complexity advantages over nonparametric techniques. Subspace methods can be used to recover the channel parameters [116], provided accurate sample-based covariance matrices can be constructed. Alternatively, by expressing the received signal in an appropriate basis, the sparsity of the channel can be made explicit, enabling the use efficient techniques from compressed sensing [134]. In particular, we express $\mathbf{a}_t(\boldsymbol{\theta}_l) = \mathbf{U}_r^{\mathrm{H}}\mathbf{a}_s$, where $\mathbf{U}_r \in N_r \times D_r$ is a dictionary matrix containing candidate responses and

$\mathbf{a}_s \in \mathbb{C}^{D_r}$ is a vector of coefficients. If one of the columns in $\mathbf{U}_r$ is equal to $\mathbf{a}_t(\theta_l)$, then $\mathbf{a}_s$ is 1-sparse. If $\mathbf{U}_r$ is full rank and $\mathbf{a}_t(\theta_l)$ is close to one of the columns (which is the case for sufficiently large N_r with $\mathbf{U}_r$ a DFT matrix and uniform linear arrays), then $\mathbf{a}_s$ is approximately 1-sparse. Applying such DFT matrices, we can express

$$\sum_{l=0}^{L-1} \rho_l e^{j\psi_l} \mathbf{a}_r(\theta_l)\, \mathbf{a}_t^{\mathrm{H}}(\phi_l)\, e^{-j2\pi\tau_l \frac{n}{N_s T_s}} = \mathbf{U}_r^{\mathrm{H}} \mathbf{H}_s[n]\, \mathbf{U}_t \tag{37}$$

where the $N_r \times N_t$ matrix $\mathbf{H}_s[n]$ is approximately L-sparse, with entries depending on the channel gains and the path delays. Introducing $\mathbf{h}_s[n] = \mathrm{vec}(\mathbf{H}_s[n])$ and substituting (37) into (28), we can write

$$\mathbf{y}[n] = \left(\mathbf{s}^{\mathrm{T}} \mathbf{F}^{\mathrm{T}}[n]\, \mathbf{U}_t^{\mathrm{T}}\right) \otimes \left(\mathbf{W}^{\mathrm{H}}[n]\, \mathbf{U}_r^{\mathrm{H}}\right) \mathbf{h}_s[n] + \mathbf{W}[n]^{\mathrm{H}} \mathbf{v}[n]. \tag{38}$$

In (38), we recognize the standard noisy compressed sensing expression $\mathbf{y}[n] = \mathbf{A}[n]\, \mathbf{h}_s[n] + \mathbf{w}[n]$, where $\mathbf{A}[n]$ is a known measurement matrix and $\mathbf{h}_s[n]$ is an approximately sparse unknown, and $\mathbf{w}[n]$ is an unknown error term [135]. Since the sparsity pattern (the support of $\mathbf{h}_s[n]$) depends on the AOAs and AODs, it is independent on the carrier index n, at least for moderate bandwidths. Hence, the vectors $\mathbf{h}_s[n]$, $n \in \{0, 1, \ldots, N_s - 1\}$, are jointly sparse, which is also standard model in compressed sensing, for which efficient recovery techniques exist [136]. Such techniques can provide estimates of the number of paths, and, for each path, an estimate of the AOA and AOD (in the form of the indices in the vector $\mathbf{h}_s[n]$). From these it is then relatively straightforward to determine the path delays and gains [126]. In practice, paths may not be specular and have a certain spread in angle and delay domain. This spread will reduce the quality of the estimates but can be considered as a separate parameter to be estimated [137]. We will denote by $\hat{\boldsymbol{\eta}} \in \mathbb{R}^{3L}$ the vector of the estimated L TOAs, AOAs, and AODs, as provided by a channel estimation routine. The corresponding true values are denoted by $\boldsymbol{\eta} \in \mathbb{R}^{3L}$, assuming no nonexisting paths were estimated.

Once the channel parameters have been estimated, we can localize the receiver. We discard the channel gains, leaving us with $\hat{\boldsymbol{\eta}} = \boldsymbol{\eta} + \mathbf{w}$, where $\mathbf{w}$ represents the statistical estimation error, here modeled as zero-mean Gaussian with covariance $\boldsymbol{\Sigma}_{\mathrm{w}}$. Denoting by $\mathbf{z}$ the location and orientation of the receiver, as well as the locations of the scatterers (all in the frame of reference of the transmitter), $\boldsymbol{\eta}$ is a deterministic injective function of $\mathbf{z}$, $\boldsymbol{\eta} = \mathbf{f}(\mathbf{z})$, $\mathbf{f} : \mathbb{R}^{2L+1} \to \mathbb{R}^{3L}$. Due to the nonlinear nature of $\mathbf{f}(\cdot)$, inference regarding $\mathbf{z}$ can be performed using a particle representation. Let $p_{\eta}(\boldsymbol{\eta}|\hat{\boldsymbol{\eta}})$ be the known distribution of the channel parameters based on the received waveforms, and $p_{\mathbf{z}}(\mathbf{z}|\hat{\boldsymbol{\eta}})$ the corresponding unknown distribution in the location space. Based on N_p samples from a well-chosen proposal distribution $\mathbf{z}^{(p)} \sim q_{\mathbf{z}}(\mathbf{z})$, a particle representation of $p_{\mathbf{z}}(\mathbf{z})$ is given by $\left\{\mathbf{z}^{(p)}, w^{(p)}\right\}_{p=1}^{N_p}$, where

$$w^{(p)} \propto \frac{p_{\eta}\left(\mathbf{f}(\mathbf{z}^{(p)})|\hat{\boldsymbol{\eta}}\right)}{q_{\mathbf{z}}\left(\mathbf{z}^{(p)}\right)}. \tag{39}$$

Based on the moments of $\{\mathbf{z}^{(p)}, w^{(p)}\}_{i=1}^{N_p}$, a new, refined, proposal distribution can be formulated. Choices for the proposal distribution in LOS and NLOS scenarios were discussed in [138].

2) Network Level: A powerful Bayesian approach in to estimate the locations and orientations of multiple nodes is the use of message passing and factor graphs [6], [139], as it can exploit the inherent structure of the problem and allow multiple agents to help each other, even in the absence of interagent measurements. Consider a scenario (see Fig. 14) with N nodes, a set of directed links $(i,j) \in \mathcal{E}$ with L_{ij} paths, and K reflectors and scatterers. The posterior distribution can be expressed as

$$p\left(\{\mathbf{x}_i, \alpha_i\}_{i=1}^{N}, \{\mathrm{R}_k\}_{k=1}^{K} | \hat{\boldsymbol{\eta}}\right) \propto \prod_{k=1}^{K} p(\mathrm{R}_k) \prod_{i=1}^{N} p(\mathbf{x}_i) p(\alpha_i) \times \prod_{(i,j)\in\mathcal{E}} \prod_{l=1}^{L_{ij}} p\left(\hat{\boldsymbol{\eta}}_i^{(l)} | \mathbf{x}_i, \alpha_i, \mathbf{x}_j, \alpha_j, \mathrm{R}_{k(l)}\right) \tag{40}$$

in which $\hat{\boldsymbol{\eta}}$ contains all the estimated channel parameters (i.e., AOA, AOD, TOA for each path of each link), $hat\,\boldsymbol{\eta}_i^{(l)}$ are the estimated parameters of path l of link (i,j), and $\mathrm{R}_{k(l)}$ is the state of reflector/scatterer $k(l)$, which is associated with path l of link (i,j) (with $\mathrm{R}_{k(l)} = \emptyset$ for LOS paths). The type of R_k depends on the scenario: with point scatterers (which were considered in the derivations in Section IV-C1), R_k is the location of the scattering point; for reflecting surfaces, R_k is a virtual anchor [119], [122] or a virtual agent. Surfaces can also be described through a point and a vector (normal or parallel to the surface) [140]. Consider an example with two agents (UE1 and UE2) with a downlink transmission from a common reference station (BS), as well as a transmission from UE2 to UE1, and a single reflector (described by state R). The factor graph of (40) corresponding to such a scenario is shown in Fig. 14. Suitable distributed message passing methods can be then developed, whereby agents collaboratively estimate their position and orientation, as well as a map of the environment. The associated factor graph can also be extended to include data association (i.e., determining which path l corresponds to which reflector/scatterer R_k) [141].

As an alternative to the model (40), one can also create a factor graph at a higher level of abstraction, as in: based on the link-level measurements, node i has an estimate of $\mathbf{R}_{\alpha_i}\left(\mathbf{x}_i - \mathbf{x}_j\right)$ and $\alpha_i - \alpha_j$. As orientations are bounded and periodic, it is preferred to treat them separately from the position in terms of the error model. Hence, a reasonable

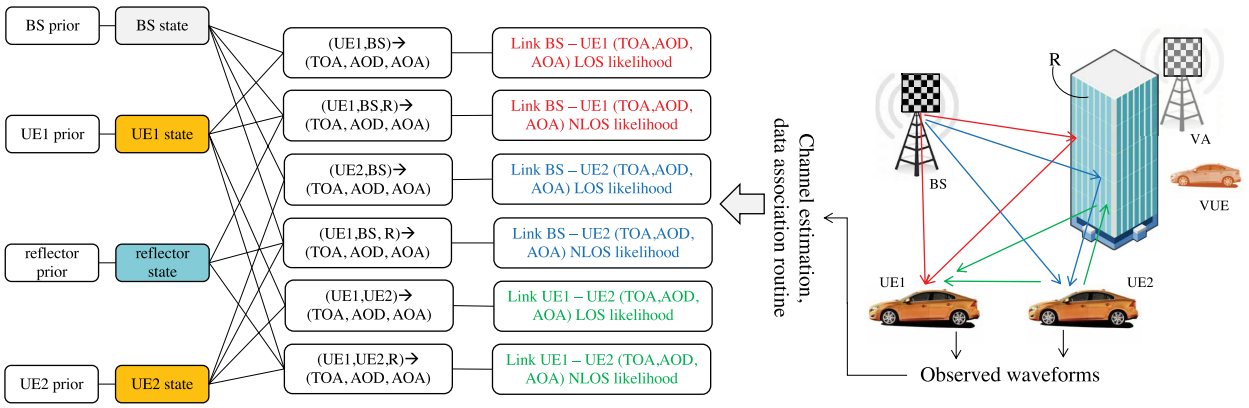

Fig. 14. ***Model and sketch of factor graph corresponding to the factorization (40), with two agents (UE1 and UE2), a base station (BS), and a reflecting surface (R), and three transmissions: downlink transmission from the BS to UE1 and UE2, and a sidelink transmission from UE2 to UE1. This leads to two virtual transmitters: a virtual anchor (VA) and a virtual use (VUE). The function with the arrow describes the deterministic mapping from the location parameters to the channel parameters.***

measurement model is Gaussian for the relative position estimate and a circular Gaussian distribution (also known as a von Mises distribution) for the relative orientation estimate:

$$p\left(\mathbf{y}_{ij}^{(\mathrm{pos})}\,|\,\mathbf{x}_i,\mathbf{x}_j,\alpha_i\right) \propto \exp\Bigg(-\frac{1}{2}\left(\mathbf{y}_{ij}^{(\mathrm{pos})}-\mathbf{R}_{\alpha_i}\left(\mathbf{x}_i-\mathbf{x}_j\right)\right)^{\mathrm{T}} \times \Sigma_{ij}^{-1}\left(\mathbf{y}_{ij}^{(\mathrm{pos})}-\mathbf{R}_{\alpha_i}\left(\mathbf{x}_i-\mathbf{x}_j\right)\right)\Bigg) \tag{41}$$

$$\log p\left(y_{ij}^{(\mathrm{or})}\,|\,\alpha_i,\alpha_j\right) \propto \exp\left(\Re\left\{a_{ij}e^{j(\alpha_i-\alpha_j)}\right\}\right) \tag{42}$$

where $a_{ij}=\exp(-jy_{ij}^{(\mathrm{or})})/\sigma_{o,ij}^2$. Here, Σ_{ij} is the covariance associated with relative location estimation and $\sigma_{o,ij}^2$ is the variance associated with relative orientation estimation. While this decoupling of the uncertainties is suboptimal, it facilitates the design of localization algorithms. Due to the nonlinearities in (41) and (42) and the coupling between position and orientation, a distributed network localization method is not obvious. We now first treat the case where locations or orientations are known and then move on to the general case.

a) Known orientations or locations: When all the nodes' orientations are known, the network localization can be formulated as

$$\underset{\mathbf{x}_1,\ldots,\mathbf{x}_N}{\text{minimize}} \sum_{(i,j)\in\mathcal{E}}\left(\mathbf{y}_{ij}^{(\mathrm{pos})}-\left(\mathbf{x}_i-\mathbf{x}_j\right)\right)^{\mathrm{T}}\Sigma_{ij}^{-1}\left(\mathbf{y}_{ij}^{(\mathrm{pos})}-\left(\mathbf{x}_i-\mathbf{x}_j\right)\right) \tag{43}$$

which is a standard convex quadratic program, and can be solved efficiently. On the other hand, when instead the locations are known but the orientations unknown, the network orientation algorithm is

$$\underset{\alpha_1,\ldots,\alpha_N}{\text{maximize}} \sum_{(i,j)\in\mathcal{E}}\frac{\cos\left(y_{ij}^{(\mathrm{or})}-\alpha_i+\alpha_j\right)}{\sigma_{o,ij}^2} \tag{44}$$

which is not convex. However, for small values of $\sigma_{o,ij}^2$, we can approximate

$$\cos\left(y_{ij}^{(\mathrm{or})}-\alpha_i+\alpha_j\right)\approx\frac{-\left(y_{ij}^{(\mathrm{or})}-\alpha_i+\alpha_j\right)^2}{2},$$

which leads again to a quadratic program.

b) Unknown orientations and locations: When the orientations are unknown, the collaborative localization problem becomes intractable to solve optimally. Message passing methods are a powerful and decentralized alternative, previously used for localization in [6] and [139]. We impose a prior distribution for each node $p(\mathbf{x}_i)p(\alpha_i)$, which for anchors reverts to a Dirac delta distribution over space and/or orientation. Collecting all measurements in a vector $\mathbf{y}$, the joint distribution of all locations and all orientations factorizes as

$$\begin{aligned} p\left(\mathbf{x}_1,\ldots,\mathbf{x}_N,\alpha_1,\ldots,\alpha_N\,|\,\mathbf{y}\right) &\propto \prod_{i=1}^{N}p(\mathbf{x}_i)p(\alpha_i)\prod_{j:(i,j)\in\mathcal{E}}p\left(\mathrm{y}_{ij}^{(\mathrm{or})}\,|\,\alpha_i,\alpha_j\right)p\left(\mathrm{y}_{ji}^{(\mathrm{or})}\,|\,\alpha_i,\alpha_j\right) \\ &\times p\left(\mathbf{y}_{ij}^{(\mathrm{pos})}\,|\,\mathbf{x}_i,\mathbf{x}_j,\alpha_i\right)p\left(\mathbf{y}_{ji}^{(\mathrm{pos})}\,|\,\mathbf{x}_j,\mathbf{x}_i,\alpha_j\right). \end{aligned} \tag{45}$$

We can now obtain approximation of the marginal posteriors $p(\mathbf{x}_i|\mathbf{y})$, $p(\alpha_i|\mathbf{y})$, or $p(\mathbf{x}_i,\alpha_i|\mathbf{y})$ through message passing over a factor graph representation of (45). While there are multiple ways to express (45) in a factor graph, we here highlight two versions.

1) In the first version, we introduce for each link in the network a likelihood function

$$\begin{aligned}\Psi_{ij}\left(\mathbf{x}_i,\alpha_i,\mathbf{x}_j,\alpha_j\right) &= p\left(\mathbf{y}_{ij}^{(\mathrm{pos})}\,|\,\mathbf{x}_i,\mathbf{x}_j,\alpha_i\right)p\left(\mathbf{y}_{ji}^{(\mathrm{pos})}\,|\,\mathbf{x}_j,\mathbf{x}_i,\alpha_j\right) \\ &\times p\left(\mathrm{y}_{ij}^{(\mathrm{or})}\,|\,\alpha_i,\alpha_j\right)\,p\left(\mathrm{y}_{ji}^{(\mathrm{or})}\,|\,\alpha_i,\alpha_j\right)\end{aligned}$$

with the understanding that some of these factors may not be present in the case of asymmetric measurements. Message passing involves the iterative approximation of $p(\mathbf{x}_i,\alpha_i|\mathbf{y})$ by beliefs

$$b^{(t)}(\mathbf{x}_i,\alpha_i)\propto p(\mathbf{x}_i,\alpha_i)\prod_{j\in\mathcal{V}_i}\mu_{j\to i}^{(t-1)}(\mathbf{x}_i,\alpha_i) \tag{46}$$

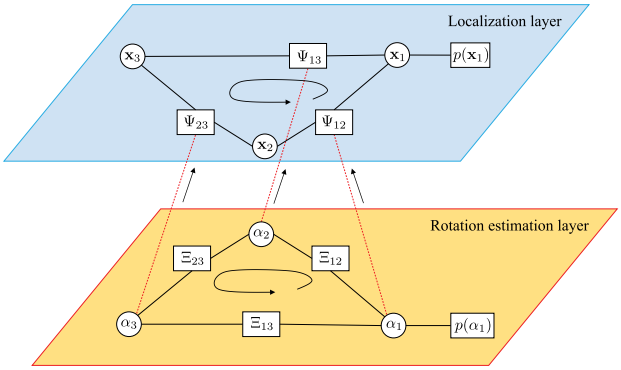

Fig. 15. ***Layered factor graph for joint localization and rotation estimation with two agents and one anchor. We introduce*** $\Xi_{ij} = p(y_{ij}^{(or)} | \alpha_i, \alpha_j) p(y_{ji}^{(or)} | \alpha_i, \alpha_j)$ ***and*** $\Psi_{ij} = \Psi_{ij}^{(pos)}(\mathbf{x}_i, \mathbf{x}_j)$***. After performing rotation estimation, messages to the localization layer are computed, and then cooperative localization is performed.***

where t is the iteration index and we have introduced message from node j to node $i \in \mathcal{V}_j$

$$\mu_{j\to i}^{(t)}(\mathbf{x}_i, \alpha_i) \propto \iint \Psi_{ij}(\mathbf{x}_i, \alpha_i, \mathbf{x}_j, \alpha_j) \frac{b^{(t)}(\mathbf{x}_j, \alpha_j)}{\mu_{i\to j}^{(t-1)}(\mathbf{x}_j, \alpha_j)} \times \mathrm{d}\alpha_j \mathrm{d}\mathbf{x}_j. \tag{47}$$

We initialize (46)and (47) by $b^{(0)}(\mathbf{x_i}, \alpha_i) = p(\mathbf{x}_i)$ $p(\alpha_i)$ and $\mu_{i\to j}^{(0)}(\mathbf{x}_j, \alpha_j) \propto 1$ and pass messages according to a given schedule (in general, a schedule whereby nodes send messages only when their beliefs are sufficiently concentrated).

2) In the second version, we harness the fact that the network orientation problem can be solved by considering only (42). Separating in (45) factors that depend on the orientation, we obtain a layered factor graph as shown in Fig. 15, for a three-node network. Performing message passing in the orientation estimation layer[9] leads to beliefs $b(\alpha_i) \approx p\left(\alpha_i | \mathbf{y}^{(\mathrm{or})}\right)$, where $\mathbf{y}^{(\mathrm{or})}$ collects all relative orientation estimates. Modeling $p(\alpha_i)$ by a von Mises distribution, it is easy to show that message passing in the orientation estimation layer involves only von Mises distributions, with parameters that can be computed in closed form. Then, each node i has a fixed $b(\alpha_i)$, and we can compute the marginalized likelihoods

$$\Psi_{ij}^{(\mathrm{pos})}(\mathbf{x}_i, \mathbf{x}_j) = \int p\left(\mathbf{y}_{ij}^{(\mathrm{pos})} | \mathbf{x}_i, \mathbf{x}_j, \alpha_i\right) b(\alpha_i) \mathrm{d}\alpha_i \times \int p\left(\mathbf{y}_{ji}^{(\mathrm{pos})} | \mathbf{x}_j, \mathbf{x}_i, \alpha_j\right) b(\alpha_j) \mathrm{d}\alpha_j$$

so that the localization algorithm operates completely in the position space

$$\mu_{i\to j}^{(t)}(\mathbf{x}_j) \propto \int \Psi_{ij}^{(\mathrm{pos})}(\mathbf{x}_i, \mathbf{x}_j) \frac{b^{(t)}(\mathbf{x}_i)}{\mu_{j\to i}^{(t-1)}(\mathbf{x}_i)} \mathrm{d}\mathbf{x}_i \tag{48}$$

[9]Under sufficiently good orientation measurements, this can be accomplished efficiently by Gaussian message passing.

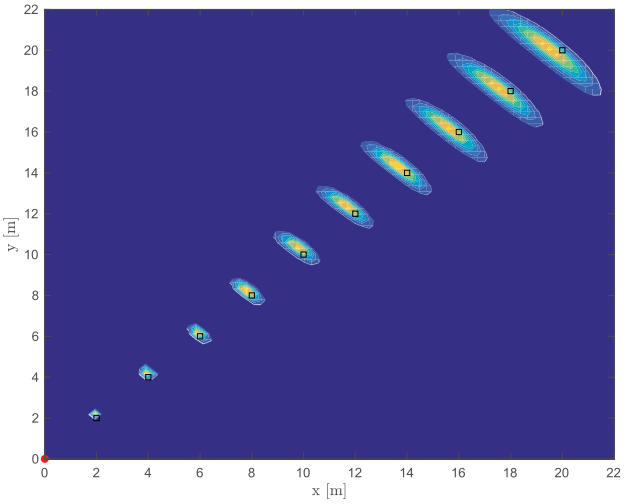

Fig. 16. ***Example outcome of joint localization and orientation estimation for a linear network. The location beliefs for individual agents are scaled and added for visualization purposes. The agents' locations are shown with a black square.***

$$b^{(t)}(\mathbf{x}_i) \propto p(\mathbf{x}_i) \prod_{j\in\mathcal{V}_i} \mu_{j\to i}^{(t-1)}(\mathbf{x}_i). \tag{49}$$

Here, $\Psi_{ij}^{(\mathrm{pos})}(\mathbf{x}_i, \mathbf{x}_j)$ plays a similar role as the ranging likelihood function $p(\hat{d}_{ij} | \| \mathbf{x}_i - \mathbf{x}_j \|)$ in range-based localization.

An example of the second approach for a linear network with one anchor at $[0, 0]^{\mathrm{T}}$ and six agents, located at $\mathbf{x}_i = [2i, 2i]^{\mathrm{T}}$ with $\alpha_i = 0$, $i \in \{1, \ldots, 6\}$, $\sigma_o = 0.2$ rad, $\Sigma = \mathrm{diag}\left(\sigma_p^2, \sigma_p^2\right)$, $\sigma_p = 0.1$ m is shown in Fig. 16. We observe two phenomena. First, agents farther away from the anchor have more location uncertainty (see also Fig. 12), as it accumulates over the network. Second, agents farther away from the anchor have more orientation uncertainty, which leads to a spreading out of the belief in the lateral direction. If the orientations were all known, the lateral uncertainty would reduce to the level of the longitudinal uncertainty. Observe the similarity between the algorithm performance in Fig. 16 and the performance bounds in Fig. 13.

E. Impairments and Practical Considerations

Many practical considerations are inherited from range-based localization, as detailed in Section III-D. Nevertheless, mmWave localization has certain specific challenges.

1) Mobility and NLOS Propagation: While our discussion pertained to static nodes, the methods from Section IV-D are readily extended to a mobile scenario, by using a separation of time scales and a mobility model for agents and anchors, connecting factor graphs over time [142]. Moreover, prior information can help with link-level processing, as was explored in [112]. In mobile scenarios, NLOS tracking can improve localization quality. Due to the ability to localize incidence points, techniques from multipath-aided localization can be applied

[119], [122]. Such techniques map and track virtual anchors, whose locations can aid other nodes traversing the same area. Generalization of methods from multisensor, multitarget tracking [143] as well as of simultaneous localization and mapping [144] to a distributed and collaborative setting are needed.

2) Signal Design: Particular to the mmWave context is the design and adaptation of beamforming. Although our results indicate that using MIMO is beneficial for coverage, it may not be possible to have a single radio frequency (RF) chain per antenna and intelligent precoding and combining strategies are needed. In the absence of prior location information, initial access procedures can be used to rapidly explore the propagation environment and determine dominant paths [145]. When prior information is available, beamforming and beam tracking can be optimized to direct sufficient energy toward incidence points and the intended receiver. Here, we can again rely on the extensive research in the mmWave community [133], [146], [147]. Related to precoding is the design of dedicated waveforms [148] and positioning reference signals [149], accounting for estimation of both range and angles. This also includes the allocation of bandwidth and time for the purpose of positioning. We foresee that since location information changes at a slow time scale, sending positioning reference signals every 100 ms is sufficient for most applications. Finally, it is still an open question whether positioning will be performed in uplink, downlink, or sidelink.

3) Synchronization: In our developments, we have assumed that all nodes have a common time basis. In practice, each node will have a local clock, characterized by a skew and an offset, both of which affect the link-level measurements. Moreover, each node will be equipped with multiple arrays [150], which must be calibrated and synchronized to a common device clock. Hence, both interdevice and intradevice synchronization can cause localization errors. Link-level synchronization can be achieved through round-trip protocols [151], but may require adaptation to fully exploit the AOA and AOD estimation at both sides of the link. Anchor-level synchronization, which in LTE base stations is performed with the help of GPS signals, may not be possible in 5G. In particular, 5G dense cells may not be in GPS coverage and may be mobile, thus needing novel synchronization approaches, both for localization and communication [152]. Network-level synchronization can also be applied, which involves joint estimation of locations, orientations, and clock parameters, as in [107] and [153]. By formulating this joint estimation problem in a factor graph, a distributed solution may be possible.

V. CONCLUSION

Radio waves are an invaluable resource for localization, with examples including LORAN, GPS, UWB, cellular systems, and WiFi. With the advent of IoT and 5G, we expect an exponential increase in the number of connected devices. Many of these devices will be equipped with D2D communication capabilities, which can be utilized for D2D location-based measurements. Hence, IoT and 5G will result in a unique opportunity for collaborative localization. We have covered the main properties of collaborative localization in both contexts. For IoT, range-based localization was identified as a promising approach. From both theoretical and algorithmic perspectives, internode collaboration provides significant performance benefits, when NLOS propagation is properly handled. Due to the nonconvex nature of the localization problem, a large number of approximate algorithms for both static and mobile nodes have been developed, many of which we compared and contrasted. Challenges such as multipath/NLOS propagation, noise variance knowledge, and device synchronization were discussed in depth. For 5G, especially in mmWave band, the combination of large available bandwidths and large antenna arrays allow for single-anchor localization. We have shown how to perform localization at the link and network levels, as well as the possibility to map the propagation environment. Specific emphasis was placed on distributed localization methods. The challenges of NLOS propagation and synchronization from IoT localization remain, but are here further exacerbated due to the specific nature of mmWave communication.

If the practical challenges in IoT and 5G localization can be solved and standardization efforts see the value of interdevice measurements, we will enter a new era of collaborative localization, with coverage and accuracies that surpass current levels by at least an order of magnitude. ■

Acknowledgment

R. M. Buehrer would like to thank collaborators S. Venkatesh, T. Jia, B. Thompson, J. Schloemann, and C. O'Lone. H. Wymeersch would like to thank M. Fröhle, N. Garcia, G. Garcia, R. Mendrzik, Z. Abu-Shaban, and G. Seco-Granados for fruitful discussions and proofreading.

REFERENCES

[1] B. W. Parkinson, J. J. Spilker, Jr., P. Axelrad, and P. Enge, Eds., *Global Positioning System: Theory and Applications*. Washington, DC, USA: AIAA, 1995.

[2] K. Ranta-Aho, "Performance of 3GPP Rel-9 LTE positioning methods," in *Proc. 2nd Invitational Workshop Opportunistic RF Localization Next Generat. Wireless Devices*, Jun. 2010, pp. 1–5.

[3] S. Gezici *et al.*, "Localization via ultra-wideband radios: A look at positioning aspects for future sensor networks," *IEEE Signal Process. Mag.*, vol. 22, no. 4, pp. 70–84, Jul. 2005.

[4] R. Zekavat and R. M. Buehrer, Eds., *Handbook of Position Location: Theory, Practice and Advances*. Hoboken, NJ, USA: Wiley, 2011.

[5] N. Patwari, J. N. Ash, S. Kyperountas, A. O. Hero, III, R. L. Moses, and N. S. Correal, "Locating the nodes: Cooperative localization in wireless sensor networks," *IEEE Signal Process. Mag.*, vol. 22, no. 4, pp. 54–69, Jul. 2005.

[6] H. Wymeersch, J. Lien, and M. Z. Win, "Cooperative localization in wireless networks," *Proc. IEEE*, vol. 97, no. 2, pp. 427–450, Feb. 2009.

[7] R. M. Buehrer and T. Jia, "Collaborative position location," in *Handbook of Position Location: Theory, Practice and Advances*, R. Zekavat and R. M. Buehrer, Eds. Hoboken, NJ, USA: Wiley, 2011.

[8] R. M. Vaghefi and R. M. Buehrer, "Cooperative RF pattern matching positioning for LTE cellular systems," in *Proc. IEEE PIMRC*, Sep. 2014, pp. 264–269.

[9] R. M. Vaghefi and R. M. Buehrer, "Improving positioning in LTE through

collaboration," in *Proc. 11th Workshop Positioning, Navigat. Commun. (WPNC)*, Mar. 2014, pp. 1–6.

[10] J. Schloemann and R. M. Buehrer, "On the value of collaboration in location estimation," *IEEE Trans. Veh. Technol.*, vol. 65, no. 5, pp. 3585–3596, May 2016.

[11] Y. Shen, H. Wymeersch, and M. Z. Win, "Fundamental limits of wideband localization—Part II: Cooperative networks," *IEEE Trans. Inf. Theory*, vol. 56, no. 10, pp. 4981–5000, Oct. 2010.

[12] G. Giorgetti, S. K. S. Gupta, and G. Manes, "Understanding the limits of RF-based collaborative localization," *IEEE/ACM Trans. Netw.*, vol. 19, no. 6, pp. 1638–1651, Dec. 2011.

[13] W. Dai, Y. Shen, and M. Z. Win, "Distributed power allocation for cooperative wireless network localization," *IEEE J. Sel. Areas Commun.*, vol. 33, no. 1, pp. 28–40, Jan. 2015.

[14] W. Dai, Y. Shen, and M. Z. Win, "A computational geometry framework for efficient network localization," *IEEE Trans. Inf. Theory*, vol. 64, no. 2, pp. 1317–1339, Feb. 2018.

[15] D. B. Jourdan and N. Roy, "Optimal sensor placement for agent localization," *ACM Trans. Sensor Netw.*, vol. 4, no. 3, pp. 128–139, Apr. 2008.

[16] K. Das and H. Wymeersch, "Censoring for Bayesian cooperative positioning in dense wireless networks," *IEEE J. Sel. Areas Commun.*, vol. 30, no. 9, pp. 1835–1842, Oct. 2012.

[17] S. M. Kay, *Fundamentals of Statistical Signal Processing: Estimation Theory*. Upper Saddle River, NJ, USA: Prentice-Hall, 1993.

[18] Y. Shen and M. Z. Win, "Fundamental limits of wideband localization—Part I: A general framework," *IEEE Trans. Inf. Theory*, vol. 56, no. 10, pp. 4956–4980, Oct. 2010.

[19] Y. Qi, H. Kobayashi, and H. Suda, "Analysis of wireless geolocation in a non-line-of-sight environment," *IEEE Trans. Wireless Commun.*, vol. 5, no. 3, pp. 672–681, Mar. 2006.

[20] D. B. Jourdan, D. Dardari, and M. Z. Win, "Position error bound for UWB localization in dense cluttered environments," in *Proc. IEEE ICC*, vol. 8. Jun. 2006, pp. 3705–3710.

[21] Y. Qi and H. Kobayashi, "On relation among time delay and signal strength based geolocation methods," in *Proc. IEEE Global Telecommun. Conf. (GLOBECOM)*, vol. 7. Dec. 2003, pp. 4079–4083.

[22] R. M. Vaghefi and R. M. Buehrer, "Cooperative sensor localization with NLOS mitigation using semidefinite programming," in *Proc. IEEE WPNC*, Mar. 2012, pp. 13–18.

[23] P. J. Voltz and D. Hernandez, "Maximum likelihood time of arrival estimation for real-time physical location tracking of 802.11a/g mobile stations in indoor environments," in *Proc. Position Location Navigat. Symp. (IEEE Cat. No.04CH37556) PLANS*, Apr. 2004, pp. 585–591.

[24] D. Dardari, C.-C. Chong, and M. Z. Win, "Improved lower bounds on time-of-arrival estimation error in realistic UWB channels," in *Proc. IEEE Int. Conf. Ultra-Wideband*, Sep. 2006, pp. 531–537.

[25] D. Dardari and M. Z. Win, "Ziv–Zakai bound on time-of-arrival estimation with statistical channel knowledge at the receiver," in *Proc. IEEE Int. Conf. Ultra-Wideband*, Sep. 2009, pp. 624–629.

[26] N. Bulusu, J. Heidemann, and D. Estrin, "GPS-less low-cost outdoor localization for very small devices," *IEEE Pers. Commun.*, vol. 7, no. 5, pp. 28–34, Oct. 2000.

[27] L. Doherty, K. Pister, and L. El Ghaoui, "Convex position estimation in wireless sensor networks," in *Proc. IEEE Conf. Comput. Commun. (INFOCOM)*, vol. 3. Apr. 2001, pp. 1655–1663.

[28] D. Niculescu and B. Nath, "Ad hoc positioning system (APS)," in *Proc. IEEE GLOBECOM*, Nov. 2001, pp. 2926–2931.

[29] Y. Shang, W. Ruml, Y. Zhang, and M. P. J. Fromherz, "Localization from mere connectivity," in *Proc. Mobile Ad Hoc Netw. Comput. (MobiHoc)*, 2003, pp. 201–212.

[30] Y. Shang, W. Rumi, Y. Zhang, and M. Fromherz, "Localization from connectivity in sensor networks," *IEEE Trans. Parallel Distrib. Syst.*, vol. 15, no. 11, pp. 961–974, Nov. 2004.

[31] S. Lederer, Y. Wang, and J. Gao, "Connectivity-based localization of large scale sensor networks with complex shape," in *Proc. IEEE Conf. Comput. Commun. (INFOCOM)*, Apr. 2008, pp. 789–797.

[32] G. Giorgetti, S. K. S. Gupta, and G. Manes, "Optimal RSS threshold selection in connectivity-based localization schemes," in *Proc. 11th Int. Symp. Modeling, Anal. Simulation Wireless Mobile Syst. (MSWiM)*, New York, NY, USA, 2008, pp. 220–228. [Online]. Available: http://doi.acm.org/10.1145/1454503.1454543

[33] S. Capkun, M. Hamdi, and J.-P. Hubaux, "GPS-free positioning in mobile ad-hoc networks," in *Proc. Hawaii Int. Conf. Syst. Sci.*, 2001, pp. 3481–3490.

[34] J. Albowicz, A. Chen, and L. Zhang, "Recursive position estimation in sensor networks," in *Proc. IEEE Int. Conf. Netw. Protocols*, Nov. 2001, pp. 35–41.

[35] C. Savarese and J. Rabaey, "Robust positioning algorithms for distributed ad-hoc wireless sensor networks," in *Proc. USENIX Annu. Tech. Conf.*, 2002, pp. 317–327.

[36] A. Savvides, H. Park, and M. B. Srivastava, "The bits and flops of the n-hop multilateration primitive for node localization problems," in *Proc. ACM WSNA*, Sep. 2002, pp. 112–121.

[37] P. Biswas and Y. Ye, "Semidefinite programming for ad hoc wireless sensor network localization," in *Proc. ACM/IEEE IPSN*, Apr. 2004, pp. 46–54.

[38] J. Liu, Y. Zhang, and F. Zhao, "Robust distributed node localization with error management," in *Proc. ACM Int. Symp. Mobile Ad Hoc Netw. Comput. (MobiHoc)*, 2006, pp. 250–261.

[39] H. Chen, G. Wang, Z. Wang, H. C. So, and H. V. Poor, "Non-line-of-sight node localization based on semi-definite programming in wireless sensor networks," *IEEE Trans. Wireless Commun.*, vol. 11, no. 1, pp. 108–116, Jan. 2012.

[40] M. R. Gholami, L. Tetruashvili, E. G. Ström, and Y. Censor, "Cooperative wireless sensor network positioning via implicit convex feasibility," *IEEE Trans. Signal Process.*, vol. 61, no. 23, pp. 5830–5840, Dec. 2013.

[41] R. M. Vaghefi and R. M. Buehrer, "Cooperative localization in NLOS environments using semidefinite programming," *IEEE Commun. Lett.*, vol. 19, no. 8, pp. 1382–1385, Aug. 2015.

[42] R. M. Vaghefi and R. M. Buehrer, "Cooperative source node tracking in non-line-of-sight environments," *IEEE Trans. Mobile Comput.*, vol. 16, no. 5, pp. 1287–1299, May 2017.

[43] F. Gu, J. Niu, and L. Duan, "WAIPO: A fusion-based collaborative indoor localization system on smartphones," *IEEE/ACM Trans. Netw.*, vol. 25, no. 4, pp. 2267–2280, Aug. 2017.

[44] Z. Yang, X. Feng, and Q. Zhang, "Adometer: Push the limit of pedestrian indoor localization through cooperation," *IEEE Trans. Mobile Comput.*, vol. 13, no. 11, pp. 2473–2483, Nov. 2014.

[45] R. M. Vaghefi, M. R. Gholami, R. M. Buehrer, and E. G. Ström, "Cooperative received signal strength-based sensor localization with unknown transmit powers," *IEEE Trans. Signal Process.*, vol. 61, no. 6, pp. 1389–1403, Mar. 2013.

[46] J. Li, J. Conan, and S. Pierre, "Mobile terminal location for MIMO communication systems," *IEEE Trans. Antennas Propag.*, vol. 55, no. 8, pp. 2417–2420, Aug. 2007.

[47] T. He, C. Huang, B. M. Blum, J. A. Stankovic, and T. Abdelzaher, "Range-free localization schemes for large scale sensor networks," in *Proc. ACM Int. Conf. Mobile Comput. Netw. (MobiCom)*, 2003, pp. 81–95.

[48] N. Patwari, A. O. Hero, III, M. Perkins, N. S. Correal, and R. J. O'Dea, "Relative location estimation in wireless sensor networks," *IEEE Trans. Signal Process.*, vol. 51, no. 8, pp. 2137–2148, Aug. 2003.

[49] Z. Wang, S. Zheng, S. Boyd, and Y. Ye, "Further relaxations of the SDP approach to sensor network localization," Stanford Univ., Stanford, CA, USA, Tech. Rep., May 2007. [Online]. Available: http://www.stanford.edu/~yye/relaxationsdp9.pdf

[50] P. Tseng, "Second-order cone programming relaxation of sensor network localization," *SIAM J. Optim.*, vol. 18, no. 1, pp. 156–185, Feb. 2007.

[51] X. Li, "Collaborative localization with received-signal strength in wireless sensor networks," *IEEE Trans. Veh. Technol.*, vol. 56, no. 6, pp. 3807–3817, Nov. 2007.

[52] A. J. Weiss and J. S. Picard, "Network localization with biased range measurements," *IEEE Trans. Wireless Commun.*, vol. 7, no. 1, pp. 298–304, Jan. 2008.

[53] T. Jia and R. M. Buehrer, "On the optimal performance of collaborative position location," *IEEE Trans. Wireless Commun.*, vol. 9, no. 1, pp. 374–383, Jan. 2010.

[54] X. Ji and H. Zha, "Sensor positioning in wireless ad-hoc sensor networks using multidimensional scaling," in *Proc. IEEE Conf. Comput. Commun. (INFOCOM)*, vol. 4. Mar. 2004, pp. 2652–2661.

[55] J. A. Costa, N. Patwari, and A. O. Hero, III, "Distributed weighted-multidimensional scaling for node localization in sensor networks," *ACM Trans. Sensor Netw.*, vol. 2, no. 1, pp. 39–64, 2006.

[56] D. Moore, J. Leonard, D. Rus, and S. Teller, "Robust distributed network localization with noisy range measurements," in *Proc. ACM Conf. Embedded Netw. Sensor Syst.*, 2004, pp. 50–61.

[57] S. Srirangarajan, A. H. Tewfik, and Z. Q. Luo, "Distributed sensor network localization using SOCP relaxation," *IEEE Trans. Wireless Commun.*, vol. 7, no. 12, pp. 4886–4895, Dec. 2008.

[58] P. Zhang and M. Martonosi, "LOCALE: Collaborative localization estimation for sparse mobile sensor networks," in *Proc. Int. Conf. Inf. Process. Sensor Netw. (IPSN)*, Apr. 2008, pp. 195–206.

[59] T. Jia and R. M. Buehrer, "A collaborative quasi-linear programming framework for ad hoc sensor localization," in *Proc. IEEE WCNC*, Mar./Apr. 2008, pp. 2379–2384.

[60] V. N. Ekambaram, K. Ramchandran, and R. Sengupta, "Collaborative high-accuracy

localization in mobile multipath environments," *IEEE Trans. Veh. Technol.*, vol. 65, no. 10, pp. 8414–8422, Oct. 2016.

[61] S. Wang, F. Luo, X. Jing, and L. Zhang, "Low-complexity message-passing cooperative localization in wireless sensor networks," *IEEE Commun. Lett.*, vol. 21, no. 9, pp. 2081–2084, Sep. 2017.

[62] F. Meyer, O. Hlinka, H. Wymeersch, E. Riegler, and F. Hlawatsch, "Distributed localization and tracking of mobile networks including noncooperative objects," *IEEE Trans. Signal Inf. Process. Netw.*, vol. 2, no. 1, pp. 57–71, Mar. 2016.

[63] M. Sun and K. C. Ho, "Successive and asymptotically efficient localization of sensor nodes in closed-form," *IEEE Trans. Signal Process.*, vol. 57, no. 11, pp. 4522–4537, Nov. 2009.

[64] S. Basagni, M. Battelli, M. Iachizzi, C. Petrioli, and M. Salehi, "Limiting the propagation of localization errors in multi-hop wireless network," in *Proc. IEEE Pervasive Comput. Commun. Workshops*, Mar. 2006, pp. 6–11.

[65] R. M. Buehrer, S. Venkatesh, and T. Jia, "Mitigation of the propagation of localization error using multi-hop bounding," in *Proc. IEEE Wireless Commun. Netw. Conf. (WCNC)*, Mar./Apr. 2008, pp. 3009–3014.

[66] T. Jia and R. M. Buehrer, "Collaborative position location for wireless networks using iterative parallel projection method," in *Proc. IEEE GLOBECOM*, Dec. 2010, pp. 1–5.

[67] T. Jia and R. M. Buehrer, "A set-theoretic approach to collaborative position location for wireless networks," *IEEE Trans. Mobile Comput.*, vol. 10, no. 9, pp. 1264–1275, Sep. 2011.

[68] S. Venkatesh and R. M. Buehrer, "NLOS mitigation using linear programming in ultrawideband location-aware networks," *IEEE Trans. Veh. Technol.*, vol. 56, no. 5, pp. 3182–3198, Sep. 2007.

[69] J. J. Caffery, Jr., "A new approach to the geometry of TOA location," in *Proc. IEEE Veh. Technol. Conf.*, vol. 4. Sep. 2000, pp. 1943–1949.

[70] D. K. Goldenberg *et al.*, "Localization in sparse networks using sweeps," in *Proc. ACM Int. Conf. Mobile Comput. Netw. (MobiCom)*, Sep. 2006, pp. 110–121.

[71] A. A. Kannan, G. Mao, and B. Vucetic, "Simulated annealing based wireless sensor network localization," *J. Comput.*, vol. 1, no. 2, pp. 15–22, 2006.

[72] A. A. Kannan, G. Mao, and B. Vucetic, "Simulated annealing based wireless sensor network localization with flip ambiguity mitigation," in *Proc. IEEE 63rd Veh. Technol. Conf.*, vol. 2. May 2006, pp. 1022–1026.

[73] A. T. Ihler, J. W. Fisher, R. L. Moses, and A. S. Willsky, "Nonparametric belief propagation for self-localization of sensor networks," *IEEE J. Sel. Areas Commun.*, vol. 23, no. 4, pp. 809–819, Apr. 2005.

[74] R. Huang and G. V. Záruba, "Incorporating data from multiple sensors for localizing nodes in mobile ad hoc networks," *IEEE Trans. Mobile Comput.*, vol. 6, no. 9, pp. 1090–1104, Sep. 2007.

[75] S. Li, M. Hedley, and I. B. Collings, "New efficient indoor cooperative localization algorithm with empirical ranging error model," *IEEE J. Sel. Areas Commun.*, vol. 33, no. 7, pp. 1407–1417, Jul. 2015.

[76] N. Kantas, S. S. Singh, and A. Doucet, "Distributed maximum likelihood for simultaneous self-localization and tracking in sensor networks," *IEEE Trans. Signal Process.*, vol. 60, no. 10, pp. 5038–5047, Oct. 2012.

[77] J.-W. Qiu and Y.-C. Tseng, "M2M encountering: Collaborative localization via instant inter-particle filter data fusion," *IEEE Sensors J.*, vol. 16, no. 14, pp. 5715–5724, Jul. 2016.

[78] W. Chen, S. Guo, Y. Wu, and Y. Yang, "History-based multi-node collaborative localization in mobile wireless ad hoc networks," in *Proc. IEEE Int. Conf. Commun. (ICC)*, May 2016, pp. 1–6.

[79] O. Ozdemir, R. Niu, and P. K. Varshney, "Tracking in wireless sensor networks using particle filtering: Physical layer considerations," *IEEE Trans. Signal Process.*, vol. 57, no. 5, pp. 1987–1999, May 2009.

[80] T. Jia and R. M. Buehrer, "On the optimal performance of collaborative position location," *IEEE Trans. Wireless Commun.*, vol. 9, no. 1, pp. 374–383, Jan. 2010.

[81] B. Zhou and Q. Chen, "On the particle-assisted stochastic search mechanism in wireless cooperative localization," *IEEE Trans. Wireless Commun.*, vol. 15, no. 7, pp. 4765–4777, Jul. 2016.

[82] T. Jia and R. M. Buehrer, "Collaborative position location with NLOS mitigation," in *Proc. IEEE PIMRC Workshops*, Sep. 2010, pp. 267–271.

[83] R. Peng and M. L. Sichitiu, "Robust, probabilistic, constraint-based localization for wireless sensor networks," in *Proc. 2nd Annu. IEEE Commun. Soc. Conf. Sensor Ad Hoc Commun. Netw. (IEEE SECON)*, Sep. 2005, pp. 541–550.

[84] C. C.-G. Chang, W. E. Snyder, and C. Wang, "Robust localization of multiple events in sensor networks," in *Proc. IEEE SUTC*, vol. 1. Jun. 2006, pp. 1–8.

[85] T. Lv, H. Gao, X. Li, S. Yang, and L. Hanzo, "Space-time hierarchical-graph based cooperative localization in wireless sensor networks," *IEEE Trans. Signal Process.*, vol. 64, no. 2, pp. 322–334, Jan. 2016.

[86] U. Hammes and A. M. Zoubir, "Robust MT tracking based on M-estimation and interacting multiple model algorithm," *IEEE Trans. Signal Process.*, vol. 59, no. 7, pp. 3398–3409, Jul. 2011.

[87] J.-F. Liao and B.-S. Chen, "Robust mobile location estimator with NLOS mitigation using interacting multiple model algorithm," *IEEE Trans. Wireless Commun.*, vol. 5, no. 11, pp. 3002–3006, Nov. 2006.

[88] M. Nájar, J. M. Huerta, J. Vidal, and J. A. Castro, "Mobile location with bias tracking in non-line-of-sight," in *Proc. IEEE ICASSP*, May 2004, pp. 956–959.

[89] I. Guvenc and C.-C. Chong, "A survey on TOA based wireless localization and NLOS mitigation techniques," *IEEE Commun. Surveys Tuts.*, vol. 11, no. 3, pp. 107–124, 3rd Quart., 2009.

[90] R. M. Vaghefi and R. M. Buehrer, "Target tracking in NLOS environments using semidefinite programming," in *Proc. IEEE MILCOM*, Nov. 2013, pp. 169–174.

[91] R. M. Vaghefi and R. M. Buehrer, "Cooperative source node tracking in non-line-of-sight environments," *IEEE Trans. Mobile Comput.*, vol. 16, no. 5, pp. 1287–1299, May 2017.

[92] T. Wang, Y. Shen, A. Conti, and M. Z. Win, "Network navigation with scheduling: Error evolution," *IEEE Trans. Inf. Theory*, vol. 63, no. 11, pp. 7509–7534, Nov. 2017.

[93] W. Dai, Y. Shen, and M. Z. Win, "A computational geometry framework for efficient network localization," *IEEE Trans. Inf. Theory*, vol. 64, no. 2, pp. 1317–1339, Feb. 2018.

[94] S. Venkatesh and R. M. Buehrer, "Non-line-of-sight identification in ultra-wideband systems based on received signal statistics," *IET Microw., Antennas Propag.*, vol. 1, no. 6, pp. 1120–1130, Dec. 2007.

[95] S. Marano *et al.*, "NLOS identification and mitigation for localization based on UWB experimental data," *IEEE J. Sel. Areas Commun.*, vol. 28, no. 7, pp. 1026–1035, Sep. 2010.

[96] J. Borras, P. Hatrack, and N. B. Mandayam, "Decision theoretic framework for NLOS identification," in *Proc. 48th IEEE Veh. Technol. Conf.*, vol. 2. May 1998, pp. 1583–1587.

[97] I. Güvenç, C.-C. Chong, F. Watanabe, and H. Inamura, "NLOS identification and weighted least-squares localization for UWB systems using multipath channel statistics," *EURASIP J. Adv. Signal Process.*, vol. 2008, p. 271984, Dec. 2008.

[98] S. Venkatesh and R. M. Buehrer, "NLOS mitigation using linear programming in ultrawideband location-aware networks," *IEEE Trans. Veh. Technol.*, vol. 56, no. 5, pp. 3182–3198, Sep. 2007.

[99] S. Bartoletti, W. Dai, A. Conti, and M. Z. Win, "A mathematical model for wideband ranging," *IEEE J. Sel. Topics Signal Process.*, vol. 9, no. 2, pp. 216–228, Mar. 2015.

[100] F. Yin, C. Fritsche, F. Gustafsson, and A. M. Zoubir, "TOA-based robust wireless geolocation and Cramér–Rao lower bound analysis in harsh LOS/NLOS environments," *IEEE Trans. Signal Process.*, vol. 61, no. 9, pp. 2243–2255, May 2013.

[101] H. Nurminen, T. Ardeshiri, R. Piché, and F. Gustafsson, "A NLOS-robust TOA positioning filter based on a skew-t measurement noise model," in *Proc. IPIN*, 2015, pp. 1–7.

[102] D. Dardari, C.-C. Chong, and M. Z. Win, "Threshold-based time-of-arrival estimators in UWB dense multipath channels," *IEEE Trans. Commun.*, vol. 56, no. 8, pp. 1366–1378, Aug. 2008.

[103] J. Zheng and Y.-C. Wu, "Joint time synchronization and localization of an unknown node in wireless sensor networks," *IEEE Trans. Signal Process.*, vol. 58, no. 3, pp. 1309–1320, Mar. 2010.

[104] R. M. Vaghefi and R. M. Buehrer, "Cooperative joint synchronization and localization in wireless sensor networks," *IEEE Trans. Signal Process.*, vol. 63, no. 14, pp. 3615–3627, Jul. 2015.

[105] Y.-C. Wu, Q. Chaudhari, and E. Serpedin, "Clock synchronization of wireless sensor networks," *IEEE Signal Process. Mag.*, vol. 28, no. 1, pp. 124–138, Jan. 2011.

[106] I.-K. Rhee, J. Lee, J. Kim, E. Serpedin, and Y.-C. Wu, "Clock synchronization in wireless sensor networks: An overview," *Sensors*, vol. 9, no. 1, pp. 56–85, Jan. 2009.

[107] W. Yuan, N. Wu, B. Etzlinger, H. Wang, and J. Kuang, "Cooperative joint localization and clock synchronization based on Gaussian message passing in asynchronous wireless networks," *IEEE Trans. Veh. Technol.*, vol. 65, no. 9, pp. 7258–7273, Sep. 2016.

[108] M. Heidari, F. O. Akgul, and K. Pahlavan, "Identification of the absence of direct path in indoor localization systems," in *Proc.*

IEEE Int. Symp. Pers., Indoor Mobile Radio Commun. (PIMRC), Sep. 2007, pp. 1–6.

[109] G.-L. Sun and W. Guo, "Bootstrapping M-estimators for reducing errors due to non-line-of-sight (NLOS) propagation," *IEEE Commun. Lett.*, vol. 8, no. 8, pp. 509–510, Aug. 2004.

[110] M. R. Gholami, L. Tetruashvili, E. G. Strom, and Y. Censor, "Cooperative wireless sensor network positioning via implicit convex feasibility," *IEEE Trans. Signal Process.*, vol. 61, no. 23, pp. 5830–5840, Dec. 2013.

[111] X. Wang, Z. Wang, and B. O'Dea, "A TOA-based location algorithm reducing the errors due to non-line-of-sight (NLOS) propagation," *IEEE Trans. Veh. Technol.*, vol. 52, no. 1, pp. 112–116, Jan. 2003.

[112] M. Koivisto *et al.*, "Joint device positioning and clock synchronization in 5G ultra-dense networks," *IEEE Trans. Wireless Commun.*, vol. 16, no. 5, pp. 2866–2881, May 2017.

[113] A. Dammann, R. Raulefs, and S. Zhang, "On prospects of positioning in 5G," in *Proc. IEEE ICCW*, Jun. 2015, pp. 1207–1213.

[114] H. Wymeersch, G. Seco-Granados, G. Destino, D. Dardari, and F. Tufvesson, "5G mmWave positioning for vehicular networks," *IEEE Wireless Commun.*, vol. 24, no. 6, pp. 80–86, Dec. 2017.

[115] R. W. Heath, Jr., N. González-Prelcic, S. Rangan, W. Roh, and A. M. Sayeed, "An overview of signal processing techniques for millimeter wave MIMO systems," *IEEE J. Sel. Topics Signal Process.*, vol. 10, no. 3, pp. 436–453, Apr. 2016.

[116] J. Li, J. Conan, and S. Pierre, "Joint estimation of channel parameters for MIMO communication systems," in *Proc. 2nd Int. Symp. Wireless Commun. Syst.*, 2005, pp. 22–26.

[117] A. Alkhateeb and R. W. Heath, Jr., "Frequency selective hybrid precoding for limited feedback millimeter wave systems," *IEEE Trans. Commun.*, vol. 64, no. 5, pp. 1801–1818, May 2016.

[118] J. Karedal *et al.*, "A geometry-based stochastic MIMO model for vehicle-to-vehicle communications," *IEEE Trans. Wireless Commun.*, vol. 8, no. 7, pp. 3646–3657, Jul. 2009.

[119] K. Witrisal *et al.*, "High-accuracy localization for assisted living: 5G systems will turn multipath channels from foe to friend," *IEEE Signal Process. Mag.*, vol. 33, no. 2, pp. 59–70, Mar. 2016.

[120] ETSI, "5G: Study on channel model for frequencies from 0.5 to 100 GHz," Tech. Rep. 3GPP TR 38.901 Version 14.1.1 Release 14, 2017.

[121] A. A. Goulianos *et al.* (2017). "Measurements and characterisation of surface scattering at 60 GHz." [Online]. Available: https://arxiv.org/abs/1710.05631

[122] C. Gentner, T. Jost, W. Wang, S. Zhang, A. Dammann, and U.-C. Fiebig, "Multipath assisted positioning with simultaneous localization and mapping," *IEEE Trans. Wireless Commun.*, vol. 15, no. 9, pp. 6104–6117, Sep. 2016.

[123] Y. Han *et al.*, "Performance limits and geometric properties of array localization," *IEEE Trans. Inf. Theory*, vol. 62, no. 2, pp. 1054–1075, Feb. 2016.

[124] R. Mendrzik, H. Wymeersch, G. Bauch, and Z. Abu-Shaban (2017). "Harnessing NLOS components for position and orientation estimation in 5G mmWave MIMO." [Online]. Available: https://arxiv.org/abs/1712.01445

[125] A. Guerra, F. Guidi, and D. Dardari, "Position and orientation error bound for wideband massive antenna arrays," in *Proc. IEEE ICCW*, Jun. 2015, pp. 853–858.

[126] A. Shahmansoori, G. E. Garcia, G. Destino, G. Seco-Granados, and H. Wymeersch, "Position and orientation estimation through millimeter-wave MIMO in 5G systems," *IEEE Trans. Wireless Commun.*, vol. 17, no. 3, pp. 1822–1835, Mar. 2018. [Online]. Available: https://arxiv.org/abs/1702.01605

[127] F. Montorsi, S. Mazuelas, G. M. Vitetta, and M. Z. Win, "On the performance limits of map-aware localization," *IEEE Trans. Inf. Theory*, vol. 59, no. 8, pp. 5023–5038, Aug. 2013.

[128] E. Leitinger, P. Meissner, C. Rüdisser, G. Dumphart, and K. Witrisal, "Evaluation of position-related information in multipath components for indoor positioning," *IEEE J. Sel. Areas Commun.*, vol. 33, no. 11, pp. 2313–2328, Nov. 2015.

[129] Z. Abu-Shaban, X. Zhou, T. Abhayapala, G. Seco-Granados, and H. Wymeersch (2017). "Error bounds for uplink and downlink 3D localization in 5G mmWave systems." [Online]. Available: https://arxiv.org/abs/1704.03234

[130] L. Li and J. L. Krolik, "Cramer–Rao performance bounds for simultaneous target and multipath positioning," in *Proc. Asilomar Conf. Signals Syst. Comput.*, Nov. 2013, pp. 2150–2154.

[131] A. J. Weiss, "Direct position determination of narrowband radio frequency transmitters," *IEEE Signal Process. Lett.*, vol. 11, no. 5, pp. 513–516, May 2004.

[132] N. Garcia, H. Wymeersch, E. G. Larsson, A. M. Haimovich, and M. Coulon, "Direct localization for massive MIMO," *IEEE Trans. Signal Process.*, vol. 65, no. 10, pp. 2475–2487, May 2017.

[133] A. Alkhateeb, O. El Ayach, G. Leus, and R. W. Heath, Jr., "Channel estimation and hybrid precoding for millimeter wave cellular systems," *IEEE J. Sel. Topics Signal Process.*, vol. 8, no. 5, pp. 831–846, Oct. 2014.

[134] K. Venugopal, A. Alkhateeb, N. G. Prelcic, and R. W. Heath, Jr., "Channel estimation for hybrid architecture-based wideband millimeter wave systems," *IEEE J. Sel. Areas Commun.*, vol. 35, no. 9, pp. 1996–2009, Sep. 2017.

[135] E. J. Candès and M. B. Wakin, "An introduction to compressive sampling," *IEEE Signal Process. Mag.*, vol. 25, no. 2, pp. 21–30, Mar. 2008.

[136] M. F. Duarte, S. Sarvotham, D. Baron, M. B. Wakin, and R. G. Baraniuk, "Distributed compressed sensing of jointly sparse signals," in *Proc. IEEE Asilomar*, Oct./Nov. 2005, pp. 3469–3472.

[137] O. Besson and P. Stoica, "Decoupled estimation of DOA and angular spread for a spatially distributed source," *IEEE Trans. Signal Process.*, vol. 48, no. 7, pp. 1872–1882, Jul. 2000.

[138] J. Talvitie, M. Valkama, G. Destino, and H. Wymeersch, "Novel algorithms for high-accuracy joint position and orientation estimation in 5G mmWave systems," in *Proc. IEEE Globecom Workshops*, Dec. 2017, pp. 1–7.

[139] A. T. Ihler, J. W. Fisher, R. L. Moses, and A. S. Willsky, "Nonparametric belief propagation for self-localization of sensor networks," *IEEE J. Sel. Areas Commun.*, vol. 23, no. 4, pp. 809–819, Apr. 2005.

[140] J. Kulmer, E. Leitinger, S. Grebien, and K. Witrisal, "Anchorless cooperative tracking using multipath channel information," *IEEE Trans. Wireless Commun.*, vol. 17, no. 4, pp. 2262–2275, Apr. 2018.

[141] F. Meyer, P. Braca, P. Willett, and F. Hlawatsch, "A scalable algorithm for tracking an unknown number of targets using multiple sensors," *IEEE Trans. Signal Process.*, vol. 65, no. 13, pp. 3478–3493, Jul. 2017.

[142] Y. Shen, S. Mazuelas, and M. Z. Win, "Network navigation: Theory and interpretation," *IEEE J. Sel. Areas Commun.*, vol. 30, no. 9, pp. 1823–1834, Oct. 2012.

[143] R. P. S. Mahler, *Statistical Multisource-Multitarget Information Fusion*. Norwood, MA, USA: Artech House, 2007.

[144] M. Adams, B.-N. Vo, R. Mahler, and J. Mullane, "SLAM gets a PHD: New concepts in map estimation," *IEEE Robot. Autom. Mag.*, vol. 21, no. 2, pp. 26–37, Jun. 2014.

[145] M. Giordani, M. Mezzavilla, and M. Zorzi, "Initial access in 5G mmWave cellular networks," *IEEE Commun. Mag.*, vol. 54, no. 11, pp. 40–47, Nov. 2016.

[146] K. Gao *et al.*, "Beampattern-based tracking for millimeter wave communication systems," in *Proc. IEEE GLOBECOM*, Dec. 2016, pp. 1–6.

[147] J. Bae, S. H. Lim, J. H. Yoo, and J. W. Choi (2017). "New beam tracking technique for millimeter wave-band communications." [Online]. Available: https://arxiv.org/abs/1702.00276

[148] A. Dammann, T. Jost, R. Raulefs, M. Walter, and S. Zhang, "Optimizing waveforms for positioning in 5G," in *Proc. IEEE SPAWC*, Jul. 2016, pp. 1–5.

[149] X. Lin *et al.*, "Positioning for the Internet of Things: A 3GPP perspective," *IEEE Commun. Mag.*, vol. 55, no. 12, pp. 179–185, Dec. 2017.

[150] W. Hong, K.-H. Baek, Y. Lee, Y. Kim, and S.-T. Ko, "Study and prototyping of practically large-scale mmWave antenna systems for 5G cellular devices," *IEEE Commun. Mag.*, vol. 52, no. 9, pp. 63–69, Sep. 2014.

[151] Z. Sahinoglu, S. Gezici, and I. Güvenç, *Ultra-Wideband Positioning Systems*, vol. 2. Cambridge, U.K.: Cambridge Univ. Press, 2008.

[152] K. J. Zou, "Network synchronization for dense small cell networks," *IEEE Wireless Commun.*, vol. 22, no. 2, pp. 108–117, Apr. 2015.

[153] B. Etzlinger, F. Meyer, F. Hlawatsch, A. Springer, and H. Wymeersch, "Cooperative simultaneous localization and synchronization in mobile agent networks," *IEEE Trans. Signal Process.*, vol. 65, no. 14, pp. 3587–3602, Jul. 2017.

ABOUT THE AUTHORS

R. Michael Buehrer (Fellow, IEEE) joined Virginia Tech, Blacksburg, VA, USA, from Bell Labs as an Assistant Professor with the Bradley Department of Electrical and Computer Engineering in 2001. He is currently a Professor of Electrical Engineering and the Director of *Wireless @ Virginia Tech*, a comprehensive research group focusing on wireless communications. During 2009, he was a Visiting Researcher at the Laboratory for Telecommunication Sciences (LTS), a federal research lab which focuses on telecommunication challenges for national defense. While at LTS, his research focus was in the area of cognitive radio with a particular emphasis on statistical learning techniques. He has authored or coauthored over 70 journal and approximately 250 conference papers and holds 12 patents in the area of wireless communications. His current research interests include geolocation, position location networks, iterative receiver design, electronic warfare, dynamic spectrum sharing, cognitive radio, communication theory, multiple-input–multiple-output (MIMO) communications, intelligent antenna techniques, ultrawideband, spread spectrum, interference avoidance, and propagation modeling. His work has been funded by the U.S. National Science Foundation, the Defense Advanced Research Projects Agency, the U.S. Office of Naval Research, and several industrial sponsors.

Dr. Buehrer, who received the Ph.D. degree in electrical engineering from Virginia Tech in 1996, was corecipient of the Fred W. Ellersick MILCOM Award in 2010 for the best paper in the unclassified technical program. He is currently a Fellow of IEEE, so named for contributions to wideband signal processing in communications and geolocation, and an Area Editor for the IEEE Transactions on Wireless Communications. He was formerly an Associate Editor for IEEE Wireless Communications Letters, the IEEE Transactions on Vehicular Technologies, the IEEE Transactions on Wireless Communications, the IEEE Transactions on Signal Processing, and the IEEE Transactions on Education. In 2014, he received the Deans Award for Teaching Excellence, and in 2003 he was named Outstanding New Assistant Professor both from the Virginia Tech College of Engineering.

Henk Wymeersch (Member, IEEE) received the Ph.D. degree in electrical engineering/applied sciences from Ghent University, Ghent, Belgium, in 2005.

He is currently a Professor of Communication Systems at the Department of Electrical Engineering, Chalmers University of Technology, Göteborg, Sweden. Prior to joining Chalmers, he was a Postdoctoral Researcher from 2005 until 2009 with the Laboratory for Information and Decision Systems, Massachusetts Institute of Technology (MIT), Cambridge, MA, USA. His current research interests include 5G localization, cooperative algorithms, and intelligent transportation systems.

Prof. Wymeersch served as an Associate Editor for IEEE Communication Letters (2009–2013), the IEEE Transactions on Wireless Communications (since 2013), and the IEEE Transactions on Communications (since 2016).

Reza Monir Vaghefi (Member, IEEE) received the M.S. degree in communication engineering from Chalmers University of Technology, Göteborg, Sweden, in 2011 and the Ph.D. degree in electrical engineering from Virginia Tech, Blacksburg, VA, USA, in 2014.

His research interests include wireless communications and signal processing, estimation theory, convex optimization, cooperative and noncooperative localization, and sensor synchronization.

Dr. Vaghefi is currently an Associate Editor for *EURASIP Journal on Advances in Signal Processing*.